Prenatal Cannabidiol and THC Exposure Induce Sex-Specific Executive Dysfunction via Divergent Pathological Rewiring of the Adult Medial Prefrontal Cortex

Olivier Manzoni
olivier.manzoni@inserm.fr
INMED, INSERM U1249 https://orcid.org/0000-0002-5579-6208
Alba Cáceres-Rodríguez
INMED, INSERM U1249
Daniela Iezzi
INMED, INSERM U1249 https://orcid.org/0000-0003-1917-4548
Olivier Lassalle
INMED
Shuai Wang
Pascale Chavis
Aix-Marseille Université https://orcid.org/0000-0002-3038-1014

Article

Keywords: in utero, cannabidiol, delta9-tetrahydrocannabinol, cannabis, prenatal, risk assessment, prefrontal cortex; pyramidal neurons, anxiety, risk assessment, repetitive behavior

Posted Date: April 27th, 2026

DOI: https://doi.org/10.21203/rs.3.rs-9428628/v1

Additional Declarations: The authors have declared there is **NO** conflict of interest to disclose

Abstract

Prenatal cannabidiol (CBD) consumption is rapidly increasing, driven by a perception of safety relative to delta9-tetrahydrocannabinol (THC). However, the long-term neurodevelopmental risks of gestational CBD remain largely uncharacterized. Using a sex-disaggregated framework, we investigated adult (P100–140) mouse offspring following in utero exposure (GD5–18; 3 mg/kg) to THC or CBD. Executive function was evaluated through risk-assessment and repetitive behavior tasks, coupled with targeted electrophysiological mapping of medial prefrontal cortex (mPFC) Layer 5 neurons, the primary hub for approach-avoidance arbitration.

We found that prenatal cannabinoids induce divergent behavioral and physiological signatures. While increased repetitive behavior was a universal hallmark of exposure, impaired risk appraisal emerged uniquely in CBD-exposed females and was dissociated from classical anxiety. At the circuit level, THC and CBD remodeling converged on a universal ablation of endocannabinoid-mediated long-term depression (eCB-LTD). In males, CBD uniquely induced a state of synaptic rigidity: a bidirectional plasticity collapse underpinned by functional saturation, elevated AMPA/NMDA ratios, and slowed NMDAR activation kinetics. We suggest that this ceiling effect creates a top-down lock on the prefrontal output circuit, precluding the synaptic flexibility necessary for executive control. In contrast, females exhibited compound-specific reorganizations of E/I balance. CBD-exposed females developed a homeostatic scaled-up architecture that preserved net E/I balance but likely increased synaptic noise, whereas THC drove a pro-excitatory phenotype through the collapse of inhibitory control.

In conclusion, prenatal CBD exposure mirrors THC neurotoxicity by hijacking sex-specific developmental trajectories. While the loss of eCB-LTD is a universal endophenotype, divergent molecular remodeling drives distinct executive failures. This study establishes that sex-specific circuit rewiring is the primary driver of adult dysfunction, providing a critical biological framework for clinical warnings against gestational CBD use.

Introduction

The landscape of cannabis consumption is shifting rapidly. With the widening legalization of recreational and medicinal cannabis, its use among pregnant women has reached unprecedented levels, often aimed at alleviating gestational nausea, insomnia, or anxiety (1, 2). Within this context, cannabidiol (CBD), the primary non-intoxicating phytocannabinoid, has emerged as a "natural" and supposedly safe alternative to delta9-tetrahydrocannabinol (THC)(3–5).

Yet the enthusiasm surrounding CBD has grown far more quickly than the supporting neurobiological data, and while the risks of prenatal THC exposure are increasingly acknowledged, surprisingly little is known about how gestational CBD shapes the adult brain—an uncertainty that raises a quiet but genuine public health concern.

The endocannabinoid system is a master regulator of mammalian neurodevelopment, orchestrating neuronal migration, axonal pathfinding, and the refinement of synaptic circuits (3, 6, 7). Over the last decade, research into prenatal cannabinoid exposure (PCE) has identified persistent behavioral and synaptic pathologies. Specifically, work from our laboratory and others has established that PCE with THC or synthetic agonists primarily induces profound social deficits and altered socio-affective trajectories, particularly in male offspring (8–10). These social impairments have been linked to a "miswiring" of critical developmental hubs, including a hyperdopaminergic phenotype in the ventral tegmental area (11), the permanent loss of cholecystokinin-containing interneurons in the hippocampus (10), and the ablation of endocannabinoid-mediated long-term depression in the medial prefrontal cortex (mPFC) (9, 12, 13).

While the "socio-affective" consequences of perinatal THC are rather well-documented, the lasting impact of the increasingly popular CBD remains unclear. Recent studies have begun to dismantle the myth of CBD's neutrality, showing that fetal exposure can alter thermal pain sensitivity via TRPV1 receptors (14), disrupt neonatal communication (15), and impair basic problem-solving and cognitive functions in a sex-specific manner (16). Furthermore, we recently demonstrated that gestational CBD induces a permanent remodeling of the adult insular cortex and a longitudinal trajectory of increased anxiety-like behaviors (17, 18).

A key question nevertheless remains unresolved: does prenatal cannabinoid exposure disrupt the high-level executive processes required for complex environmental adaptation?

Unlike social play or basic memory, high-level executive processes—such as risk appraisal and behavioral switching—require the "top-down" integration of conflicting sensory cues and the active inhibition of reflexive responses. Whether prenatal CBD or THC disrupts the cognitive ability to evaluate approach-avoidance conflicts or to transition between motor and cognitive programs remains entirely

unknown. In the present study, we tested the hypothesis that these executive failures would be reflected in specialized behavioral readouts: the Stretched Attend Posture (SAP), an active risk-assessment behavior measuring cognitive arbitration (during elevated plus maze -EPM-) and the persistence of repetitive motor loops in the marble burying task (MB), which serves as a probe for behavioral switching. Because the mPFC, and specifically its Layer-5 pyramidal output neurons, serves as the principal engine driving these executive functions, we targeted this circuit to identify the underlying cellular substrate of the observed behavioral failures. We provide a definitive, sex-disaggregated comparison of prenatal THC and CBD, reporting that both cannabinoids induce a profound state of synaptic rigidity characterized by a bidirectional collapse of plasticity, that provides a plausible mechanistic explanation for the failure of behavioral adaptation.

Taken together, our findings show that CBD reproduces the executive and synaptic vulnerabilities long attributed to THC, revealing a common pathological signature of dysfunction that strengthens the rationale for cautioning against CBD use during pregnancy.

Materials and methods

Animals

All procedures complied with the European Communities Council Directive (86/609/EEC) and the United States NIH Guide for the Care and Use of Laboratory Animals and were approved by the French Ethical Committee (APAFIS #49376-2024051414491391 and APAFIS #49376). Male and female C57BL/6J mice (6–8 weeks old) were purchased from Charles River Laboratories and housed in standard wire-topped Plexiglas cages (42 cm 27 cm 14 cm) under temperature and humidity-controlled conditions (temperature 21 1°C, 60 10% relative humidity, and 12 h light/dark cycles). Food and water were available *ad libitum*. After one week of acclimation, female pairs were placed with a single male mouse in the late afternoon. The morning a vaginal plug was found was designated as gestational day 0 (GD0) and pregnant mice were housed individually. From GD5 to GD18, dams were injected subcutaneously (s.c.) daily with vehicle, 3 mg/kg of CBD (15, 17, 18) or 3 mg/kg of THC (16) (NIDA Drug Supply Program), dissolved in a vehicle consisting of Cremophor EL (Sigma-Aldrich), ethanol, and saline at 1:1:18 ratios, and administered at a volume of 4 mL/kg. Control dams (SHAM) were injected with the same volume of vehicle solution. These doses of CBD or THC reach the embryonic brain and induces behavioral changes in the offspring (9, 16–18). For each litter, the date of birth was designated as postnatal day (PND) 0. Pups were weaned at PND21 and housed separately by sex. Experiments were conducted in adulthood (PND90–140). Sample sizes (n) for each group are reported in the figure legends. Groups were formed from the complete offspring of 3–4 litters, as culling was not performed for ethical reasons.

Behavior

Testing

To evaluate anxiety-related and repetitive behaviors in adulthood, we employed the EPM and the MB test (20). The elevated plus maze (EPM) consisted of two open arms (30 × 5 cm) and two closed arms (30 × 5 × 12 cm) extending from a central platform (5 × 5 cm) elevated from the floor by 45 cm. Each mouse was placed on the central platform and allowed to explore for 5 min. Sessions were recorded with a camera positioned above the apparatus, and behavior was analyzed using EthoVision software (Noldus, The Netherlands). Locomotor activity was quantified as total distance traveled (cm). Anxiety-related measures included time spent in the open arms, closed arms, and center, as well as relative open-arm preference, calculated as (time in open arms / total session time – time in open arms) × 100. Postural analysis was assessed by scoring the proportion of time spent in normal, contracted, and stretched postures across the entire arena and within each maze subdivision (center, open arms, closed arms).

The marble burying (MB) test was conducted in a clean cage containing 4 cm of bedding, with 20 marbles evenly arranged on the surface in 5 rows of 4 marbles. Each mouse was placed in a corner to initiate the trial, and behavior was observed for 20 min. At the end of the session marbles covered more than two-thirds by bedding were considered as buried.

Behavioral data statistical analyses were performed using GraphPad Prism 11. Data sets were first tested for normality with the D'Agostino–Pearson and Shapiro–Wilk tests, and potential outliers were identified and excluded using the ROUT method. Differences between medians were evaluated with two-way ANOVA, followed by Sidak's multiple-comparison post-hoc tests. Statistical significance was reported as exact p values in the figures. Experimental results are described qualitatively in the main text, while full statistical details—including sample size (N), test type, and p values—are provided in the figure legends and associated tables. Quantitative data are presented as violin plots showing median, 25th–75th percentiles with individual data points superimposed as scatter plots.

Physiology

Slice Preparation: Adult male and female mice (PND 100–140) were deeply anesthetized with isoflurane and sacrificed according to institutional regulations. The brain was sliced (300 µm) in the coronal plane with a vibratome (Integraslice, Campden Instruments) in a sucrose-based solution at 4°C (in mM: 87 NaCl, 75 sucrose, 25 glucose, 2.5 KCl, 4, 0.5, 2, and 1.25) as described previously for the PFC (21–23). Immediately after cutting, slices containing the PFC were stored for 30 minutes at 32°C in a low-calcium artificial CSF (aCSF) containing (in mM): 130 NaCl, 11 glucose, 2.5 KCl, 2.4 MgCl2, 1.2 CaCl2, 23 NaHCO3, and 1.2 NaH2PO4, equilibrated with 95% O_2/CO_2 /5%, and then kept at room temperature until the time of recording.

Electrophysiology

Data were recorded with an Axopatch-200B amplifier (Molecular Devices), low-pass filtered at 2 kHz, digitized (10 kHz, DigiData 1440A, Molecular Devices), and analyzed using Clampex 10.7 (Molecular Devices). During recording, slices were placed in the recording chamber and continuously perfused at 2 mL/min with warm (32°C) low- solution using the receptor blocker gabazine 10 µM (SR 95531 hydrobromide; Tocris). Pyramidal neurons were visualized under a differential interference contrast microscope using an upright microscope with infrared illumination (Olympus). Whole-cell patch-clamp recordings were made from the soma of layer V/VI pyramidal neurons in the prelimbic PFC (21–26).

For current-clamp and voltage-clamp recordings, patch pipettes were filled with an intracellular solution containing (in mM): 145 K^+ gluconate, 3 NaCl, 1 $MgCl_2$, 1 EGTA, 0.3 $CaCl_2$, 2 Na^{2+} ATP, 0.3 Na^+ GTP, and 0.2 cAMP, buffered with 10 HEPES (pH 7.25, osmolarity 290–300 mOsm). Electrode resistance was 2–3 MΩ. Access resistance was monitored (< 25 MΩ) and the potential reference of the amplifier was adjusted to zero before breaking into the cell. Cells were held at − 70 mV. Current-voltage (I-V) curves were made by a series of hyperpolarizing to depolarizing current steps immediately after breaking into the cell.

Postsynaptic Spontaneous Activity and Evoked Plasticity: Spontaneous activity was recorded to isolate AMPA, NMDA, and GABA currents (17, 25). AMPA-sEPSCs: Recorded at − 70 mV using K-gluconate internal solution previously described with gabazine (10 µM, SR 95531 hydrobromide; Tocris). GABA-sEPSCs Recorded at -70mV in presence of 20 µM CNQX (6-Cyano-7-nitroquinoxaline-2,3-dione disodium, an AMPA receptor antagonist, Tocris) and L-APV 50 µM (DL-2-Amino-5-phosphonopentanoic acid, a selective NMDA receptor antagonist, Tocris); using a high chloride internal solution (in mM: 140 KCl, 1.6 MgCl2, 2.5 MgATP, 0.5 NaGTP, 2 EGTA, 10 HEPES). The pH solution was adjusted to 7.25–7.3 and osmolarity to 280–300 mOsm. + NMDA-sEPSCs: Recorded at + 30 mV in the presence of 20 µM NBQX (2,3-dioxo-6-nitro-7-sulfamoyl-benzo[f]quinoxaline, Tocris) to block AMPA and kainite mediated currents and using a cesium-methanesulfonate internal solution (in mM: 143 cesium-methanesulfonate, 5 NaCl, 1 $MgCl_2$, 1 EGTA, 0.3 $CaCl_2$, 10 Hepes, 2 Na2ATP, 0.3 NaGTP and 0.2 cAMP (pH 7.3 and 290 mOsm).

AMPA/NMDA Ratio

Measured on EPSCs (having AMPA-R and NMDA-R components) evoked by electrical stimulation in layer 2/3 while recording layer 5 pyramidal neurons at + 30 mV in Cs-methanesulfonate internal solution. The NMDA-R component was isolated by bath application of NBQX (20 µM) and the AMPA component obtained by digital subtraction (25).

Extracellular Recordings: Field excitatory postsynaptic potentials (fEPSP) were recorded in layer 5 by electrical stimulation on layer 2/3 at 0.1 Hz. The glutamatergic nature was confirmed using CNQX (10 µM) at the end of each recording. Stimulus intensity was set at 60% of maximal intensity after performing an input-output curve. *LTP Induction*: plasticity was induced by a Theta-burst stimulation (TBS) consisting of five trains of bursts (4 pulses at 100 Hz, 200-ms interval), repeated 4 times at 10 s intervals (25). *LTD Induction*: plasticity was induced by a 10 Hz stimulation for 10 min (22).

Data Analysis and Statistics: Data were analyzed off-line with Clampfit 11.3 and AxoGraph 1.7.6. Graphs were generated with GraphPad Prism 10.4.1. RMP was measured immediately after whole-cell formation. Membrane capacitance (Cm) was estimated by integrating the capacitive current evoked by a − 2 mV pulse, while membrane resistance was estimated from the I-V curve around resting membrane potential (RMP). The intrinsic excitability curve was made by measuring the number of action potentials elicited by depolarizing current steps of increasing amplitude, while rheobase and threshold were determined using a series of depolarizing 10 pA current steps. The frequency and amplitude of sEPSCs were analyzed with Axograph X using a double exponential template: f(t) = exp(-t/rise) + exp(-t/decay) (rise = 0.5 ms and decay = 3 ms). for AMPA-sEPSCs, rise = 0.5 ms and decay = 3 ms; for GABA-IPSCs, rise = 0.2 ms and decay = 10 ms; for NMDA-sEPSCs, rise = 3 ms and decay = 10 ms. Detection threshold was 3.5 times the baseline noise SD

(amplitude threshold 7 pA). Total charge transfer was calculated by the addition of the charge transfer of every individual event in 6 min of acquisition (17, 25, 27). For AMPA/NMDA ratios, AMPA-EPSC component was obtained by digital subtraction of the NMDA-EPSC from the dual component EPSC (AMPA/NMDA ratio = area AMPA-EPSC at + 30mV/ area NMDA-EPSC at + 30 mV). For field recording experiments, the magnitude of plasticity was calculated at 30–40 min after induction as percentage of baseline responses.

Datasets were tested for normality (D'Agostino-Pearson and Shapiro-Wilk) and outliers (ROUT test) before running parametric or non-parametric tests. Statistical significance was assessed with two-way ANOVA followed by Sidak's multiple comparison post-hoc tests. Quantitative data are presented as violin plots (median, 25th and 75th quartile) with individual data points superimposed.

Synaptic Distribution and E/I Balance Analysis

Statistical analysis was performed in R (version 4.2.2) and GraphPad Prism 10.4.1. Cumulative distributions of excitatory and inhibitory charge transfer were compared using the Kolmogorov-Smirnov (KS) test. To evaluate the net functional balance, we calculated a net E/I Index (E/[E + I]). Because E and I current were recorded from independent populations of neurons, a nonparametric bootstrap was performed in R (version 4.2.2). For each group, the vectors of E and I value were resampled 10,000 times with replacement using the sample() function. Within each bootstrap iteration, we computed the mean E and mean I, using built-in R functions, and calculated the corresponding E/I index (E/(E + I)). This procedure yielded 10,000 bootstrap estimates of the E/I index per group. To quantify between-group differences, we computed the ΔE/I index by subtracting the bootstrap distributions (i.e., Group Sham minus Group CBD or THC). The proportion of ΔE/I values greater or less than zero was then used to assess significance. Following a standard bootstrap-based criterion, distributions in which more than 95% of ΔE/I values fell on one side of zero were interpreted as significant at $p < 0.05$.

To facilitate reading and interpretation, all statistical results are compiled in tables, while the figures display only the comparisons between male and female controls and the within-sex comparisons used to assess the effects of each compound.

Results

In this study, we examined the long-term consequences of prenatal exposure to CBD and THC. To verify that gestation proceeded normally, several parameters were monitored throughout pregnancy. As shown in Table 1, pregnant dams exhibited comparable weight gain across groups, and pups were delivered around gestational day 19. Litter size and sex ratio were also unaffected. Together, these observations indicate that pregnancy progressed normally despite the daily subcutaneous cannabinoid treatment administered from gestational day 5 to 18.

Table 1
Follow up of gestational parameters and litter features. Statistical significance defined as p-value < 0.05.

Gestational parameters	Treatment	Median	Max	Min	N	*Kruskal-Wallis test (p-value)*
Gestational weight gain (grams)	SHAM	16.40	18.70	12.70	18	0.4491
	CBD	16.95	20.70	13.10	24	
	THC	16.80	19.80	11.50	9	
Duration of gestation (days)	SHAM	19.00	20.00	18.00	18	0.7293
	CBD	19.00	20.00	17.00	24	
	THC	19.00	19.00	18.00	9	
Litter size (#)	SHAM	7.00	10.00	3.00	18	0.0813
	CBD	8.00	10.00	1.00	24	
	THC	8.00	10.00	5.00	9	
Ratio males/females	SHAM	1.33	5.00	0.33	18	0.1697
	CBD	1.63	9.00	0.14	25	
	THC	0.67	4.00	0.17	9	

We employed the elevated plus maze (EPM) and marble burying (MB) to assess complementary facets of emotional and defensive behavior at adulthood. The EPM quantifies anxiety-related responses and ethological risk-assessment strategies such as stretch-attend

postures, whereas the MB test probes repetitive and defensive actions associated with anxiety and compulsivity (28, 29). Together, these paradigms provide convergent yet distinct behavioral readouts, enhancing sensitivity to cannabinoid-induced alterations and enabling us to distinguish shared from domain-specific effects of prenatal THC and CBD exposure.

Prenatal cannabinoids spare classical adult anxiety indices despite adolescent vulnerability.

Epidemiological and preclinical data suggest that *in utero* cannabis exposure increases the risk for affective disorders (2, 30–32). While we previously identified a female-specific anxiogenic-like phenotype during adolescence following prenatal CBD exposure (15, 18), we sought to determine the long-term stability of these effects and whether prenatal THC induces a convergent or divergent adult behavioral profile.

In the EPM, no significant group differences were detected by sex or prenatal exposure across canonical anxiety indices, including open-arm preference and time spent in open or closed arms (Table 2, Supplemental Fig. 1). A significant increase in total distance travelled was noted uniquely in THC-exposed females, indicating a degree of hyper-locomotion independent of affective state. Notably, the adolescent anxiogenic-like EPM phenotype previously reported in CBD females (18) was no longer evident in adulthood. These data suggest a developmental "recovery" of basal approach-avoidance behavior, consistent with prior reports of stable open-arm exploration following prenatal THC (9).

Table 2
Coventional EPM analysis. Statistical significance defined as p-value < 0.05.

Measure	Treatment	Median	Max	Min	N	*Two-way ANOVA Main effects and interactions*	*Multiple comparison (Šidák's post hoc test)*
Distance moved (cm)	SHAM FEMALE	957.618	1591.55	503.066	13	**Interaction**: F (2, 74) = 0,3939; P = 0,6758 **Sex**: F (1, 74) = 1,398; P = 0,2409 **Treatment** F (2, 74) = 4,419; P = 0,0154	FEMALE "Sham vs. CBD" P = 0,2099 "Sham vs. THC" P = 0,0250 "CBD vs. THC" P = 0,6904 MALE "Sham vs. CBD" P = 0,8485 "Sham vs. THC" P = 0,2752 "CBD vs. THC" P = 0,6260
	CBD FEMALE	1150.015	1723.54	750.624	12		
	THC FEMALE	1282.48	1661.58	899.255	16		
	SHAM MALE	1075.535	2020.9	810.543	11		
	CBD MALE	1282.85	1758.49	584.972	10		
	THC MALE	1276.36	1705.87	1012.67	16		
Preference for Open Arms (%)	SHAM FEMALE	17.39257	58.8596	0.383216	13	**Interaction**: F (2, 72) = 0,3889; P = 0,6792 **Sex**: F (1, 72) = 0,1030; P = 0,7492 **Treatment** F (2, 72) = 2,464; P = 0,0922	FEMALE "Sham vs. CBD" P = 0,9909 "Sham vs. THC" P = 0,4119 "CBD vs. THC" P = 0,5080 MALE "Sham vs. CBD" P = 0,3921 "Sham vs. THC" P = 0,1629 "CBD vs. THC" P = 0,9285
	CBD FEMALE	25.64002	49.27898	5.156046	12		
	THC FEMALE	28.300745	93.13346	7.419347	16		
	SHAM MALE	17.72665	42.86245	3.019399	11		
	CBD MALE	33.124375	55.86683	7.895273	10		
	THC MALE	33.847205	71.15472	3.166812	16		
Closed Arms + Centre (%)	SHAM FEMALE	83.4482	99.41843	62.6866	13	**Interaction**: F (2, 72) = 0,2805; P = 0,7563 **Sex**: F (1, 72) = 0,2130; P = 0,9357 **Treatment** F (2, 72) = 2,798; P = 0,0676	FEMALE "Sham vs. CBD" P = 0,9243 "Sham vs. THC" P = 0,3009 "CBD vs. THC" P = 0,5406 MALE "Sham vs. CBD" P = 0,3705 "Sham vs. THC" P = 0,1621 "CBD vs. THC" P = 0,9430
	CBD FEMALE	79.02395	93.5023	66.329	12		
	THC FEMALE	76.99995	92.7134	51.2264	16		
	SHAM MALE	84.0974	96.83627	66.5836	11		
	CBD MALE	74.4891	91.90925	63.9245	10		
	THC MALE	73.7754	95.84524	56.1791	16		
Open Arms (%)	SHAM FEMALE	15.09575	37.0318	0.387722	13	**Interaction**: F (2, 75) = 0,8071; P = 0,4500 **Sex**: F (1, 75) = 0,006545; P = 0,6458 **Treatment** F (2, 75) = 2,087; P = 0,1312	FEMALE "Sham vs. CBD" P = 0,9997 "Sham vs. THC" P = 0,7523 "CBD vs. THC" P = 0,7379 MALE
	CBD FEMALE	20.3919	33.0084	4.90141	12		
	THC FEMALE	22.04415	48.213	0.381558	16		

SHAM MALE	14.3997	29.9907	0	11	"Sham vs. CBD" P = 0,9997 "Sham vs. THC" P = 0,7523 "CBD vs. THC" P = 0,7379
CBD MALE	24.776	35.8404	7.31569	10	
THC MALE	25.2479	42.2859	3.07094	16	

Prenatal CBD, but not THC, induces enduring female-specific increases in risk-assessment postures.

To determine if prenatal cannabinoid exposure alters active exploratory strategies, we performed an ethological analysis of postural states during the EPM (Fig. 1, Table 3). Across all experimental groups, a neutral stance was the most frequent posture. Notably, females exposed to THC exhibited this neutral posture significantly more often than Sham-controls. Furthermore, a general sexual dimorphism was observed, as males consistently expressed a neutral body posture more frequently than their treatment-matched female counterparts.

Table 3
Postural analysis during EPM. Statistical significance defined as p-value < 0.05.

Measure	Treatment	Median	Max	Min	N	*Two-way ANOVA Main effects and interactions*	*Multiple comparison (Šidák's post hoc test)*
Normal posture (%)	SHAM FEMALE	76.44	85.23	68.15	13	**Interaction**: F (2, 74) = 4,760; P = 0,0114 **Sex**: F (1, 74) = 38,20; P < 0,0001 **Treatment** F (2, 74) = 11,64; P < 0,0001	**FEMALE** "Sham vs. CBD" P = 0,5584 "Sham vs. THC" P = 0,0125 "CBD vs. THC" P = 0,1842 **MALE** "Sham vs. CBD" P < 0,0001 "Sham vs. THC" P = 0,0078 "CBD vs. THC" P = 0,1059 **FEMALE vs. MALE** "Sham" P = 0,0386 "CBD" P = < 0,0001 "THC" P = 0,0103
	CBD FEMALE	77.40	84.77	71.86	12		
	THC FEMALE	80.09	88.57	77.29	16		
	SHAM MALE	80.02	84.89	72.60	11		
	CBD MALE	88.15	91.54	81.81	10		
	THC MALE	84.97	92.21	76.58	16		
Strech attend posture (%)	SHAM FEMALE	13.29	18.46	7.14	13	**Interaction**: F (2, 74) = 2,479; P = 0,0908 **Sex**: F (1, 74) = 87,79; P < 0,0001 **Treatment** F (2, 74) = 11,82; P < 0,0001	**FEMALE** "Sham vs. CBD" P = 0,0064 "Sham vs. THC" P = 0,2608 "CBD vs. THC" P < 0,0001 **MALE** "Sham vs. CBD" P = 0,9611 "Sham vs. THC" P = 0,1769 "CBD vs. THC" P = 0,1098 **FEMALE vs. MALE** "Sham" P < 0,0001 "CBD" P < 0,0001 "THC" P < 0,0001
	CBD FEMALE	18.06	23.97	7.08	12		
	THC FEMALE	11.40	16.43	6.21	16		
	SHAM MALE	7.27	11.88	4.52	11		
	CBD MALE	7.41	13.80	4.33	10		
	THC MALE	5.31	9.25	1.60	16		
Contracted posture (%)	SHAM FEMALE	8.54	22.59	4.28	13	**Interaction**: F (2, 74) = 0,7749; P = 0,4645 **Sex**: F (1, 74) = 1,642; P = 0,2040 **Treatment** F (2, 74) = 17,64; P < 0,0001	**FEMALE** "Sham vs. CBD" P = 0,0026 "Sham vs. THC" P = 0,2678 "CBD vs. THC" P = 0,0982 **MALE** "Sham vs. CBD" P < 0,0001 "Sham vs. THC" P = 0,2682 "CBD vs. THC" P = 0,0017
	CBD FEMALE	3.55	9.61	1.79	12		
	THC FEMALE	6.12	14.54	3.29	16		
	SHAM MALE	11.58	20.90	5.67	11		

CBD MALE	3.29	6.93	1.21	10	**FEMALE vs. MALE** "Sham" P = 0,2143 "CBD" P = 0,7723 "THC" P = 0,1713
THC MALE	9.26	21.82	3.84	16	

Focusing on the Stretched-Attend Posture (SAP), a key index of risk-assessment, revealed a selective vulnerability in the CBD lineage. CBD-exposed females engaged in SAP significantly longer than both Sham females and CBD-exposed males, which unveils an increased hesitation. This behavioral shift was compound-specific, as no increase in SAP was observed in THC-exposed groups. This elongation of risk-assessment was accompanied by a reciprocal reduction in contracted postures among CBD offspring, further indicating a strategy shift toward a hesitant behavior. These results establish that prenatal CBD, but not THC, selectively promotes risk-assessment behavior in adult female offspring.

We next investigated whether these postural alterations were distributed uniformly across the maze or confined to specific zones (Fig. 1, Table 4). Regardless of sex or treatment, animals spent most of their time in neutral postures within the closed arms. Notably, the increase in SAP observed in CBD-exposed females was spatially restricted; these offspring exhibited a selective enhancement of SAP while positioned in the closed arms, hesitating prior to transitioning into the center zone. This spatial bias indicates that the impact of prenatal CBD is most pronounced during the preparatory phase of exploration, where hyper-vigilance is heightened in contexts of relative safety before approaching a zone of uncertainty.

Table 4
Postural analysis during EPM per area of the maze. Statistical significance defined as p-value < 0.05.

Measure	Area	Treatment	Median	Max	Min	N	*Two-way ANOVA Main effects and interactions*	*Multiple comparison (Šidák's post hoc test)*
Normal posture (%)	**Center**	SHAM FEMALE	16.9	29.5	2.4	13	**Interaction**: F (2, 72) = 3,582; P = 0,0329 **Sex**: F (1, 72) = 0,3666; P = 0,5468 **Treatment** F (2, 72) = 0,9996; P = 0,3731	**FEMALE** "Sham vs. CBD" P = 0,9334 "Sham vs. THC" P = 0,6266 "CBD vs. THC" P = 0,8553 **MALE** "Sham vs. CBD" P = 0,2775 "Sham vs. THC" P = 0,0170 "CBD vs. THC" P = 0,5388 **FEMALE vs. MALE** "Sham" P = 0,0324 "CBD" P = 0.8552 "THC" P = 0,1212
		CBD FEMALE	17.9	26.5	10.5	12		
		THC FEMALE	18.3	36.1	9.7	16		
		SHAM MALE	26.2	34.3	3.5	11		
		CBD MALE	19.9	28.2	6.6	10		
		THC MALE	15.8	22.9	7.1	16		
	Open arms	SHAM FEMALE	10.5	30.3	0.4	13	**Interaction**: F (2, 72) = 0,5525; P = 0,5779 **Sex**: F (1, 72) = 2,863; P = 0,0949 **Treatment** F (2, 72) = 2,717; P = 0,0729	x
		CBD FEMALE	13.2	24.3	2.9	12		
		THC FEMALE	16.8	37.2	4.1	16		
		SHAM MALE	12.8	28.2	2.1	11		
		CBD MALE	20.2	32.5	5.1	10		
		THC MALE	20.5	41.6	2.4	16		
	Closed arms	SHAM FEMALE	44.6	72.2	27.3	13	**Interaction**: F (2, 72) = 0,6394; P = 0,5306 **Sex**:F (1, 72) = 0,2572; P = 0,6136 **Treatment** F (2, 72) = 0,9359; P = 0,3970	x
		CBD FEMALE	46.5	64.8	28.4	12		
		THC FEMALE	42.3	57.5	25.1	16		
		SHAM MALE	38.2	71.5	25.9	11		
		CBD MALE	47.8	79.1	36.9	10		
		THC MALE	44.3	72.9	31.1	16		
SAP(%)	**Center**	SHAM FEMALE	2.8	5.2	0.9	13	**Interaction**: F (2, 72) = 1,026; P = 0,3635 **Sex**: F (1, 72) = 84,53; P < 0,0001 **Treatment** F (2, 72) = 5,502; F (2, 72) = 5,502	**FEMALE** "Sham vs. CBD" P = 0,3855 "Sham vs. THC" P = 0,1254 "CBD vs. THC" P = 0,0040 **MALE** "Sham vs. CBD" P = 0,9995 "Sham vs. THC" P = 0,4290 "CBD vs. THC" P = 0,4662 **FEMALE vs. MALE** "Sham" P < 0,0001 "CBD" P < 0,0001 "THC" P < 0,0001
		CBD FEMALE	3.4	5.6	1.3	12		
		THC FEMALE	2.2	3.9	0.6	16		
		SHAM MALE	1.1	1.6	0.3	11		
		CBD MALE	0.9	1.9	0.2	10		
		THC MALE	0.6	2.2	0	16		
	Open arms	SHAM FEMALE	4.6	6.9	0	13	**Interaction**: F (2, 72) = 0,5450; P = 0,5822	**FEMALE**

		CBD FEMALE	6.4	8.8	1.6	12	**Sex**: F (1, 72) = 30,06; P < 0,0001 **Treatment** F (2, 72) = 3,231; P = 0,0453	"Sham vs. CBD" P = 0,0765 "Sham vs. THC" P = 0,3010 "CBD vs. THC" P = 0,6691 **MALE** "Sham vs. CBD" P = 0,3507 "Sham vs. THC" P = 0,9999 "CBD vs. THC" P = 0,2865 **FEMALE vs. MALE** "Sham" P = 0.0192 "CBD" P = 0.0044 "THC" P < 0,0001
		THC FEMALE	4.7	10.7	2.4	16		
		SHAM MALE	1.9	5.5	0.9	11		
		CBD MALE	3.2	6.5	1.2	10		
		THC MALE	1.7	5.9	0.4	16		
	Closed arms	SHAM FEMALE	5.9	8.9	3.1	13	**Interaction**: F (2, 72) = 6,353; P = 0,0029 **Sex**:F (1, 72) = 44,95; P < 0,0001 **Treatment** F (2, 72) = 17,66; P < 0,0001	**FEMALE** "Sham vs. CBD" P = 0,0220 "Sham vs. THC" P = 0,0008 "CBD vs. THC" P < 0.0001 **MALE** "Sham vs. CBD" P = 0,7360 "Sham vs. THC" P = 0,0687 "CBD vs. THC" P = 0,3558 **FEMALE vs. MALE** "Sham" P = 0.0032 "CBD" P < 0.0001 "THC" P = 0.0490
		CBD FEMALE	8.3	10.5	4.1	12		
		THC FEMALE	3.9	7.4	1.2	16		
		SHAM MALE	3.9	5.7	2.1	11		
		CBD MALE	3.1	8.1	1.3	10		
		THC MALE	2.6	5.4	0.6	16		
Contracted posture(%)	**Center**	SHAM FEMALE	0.06	0.5	0	13	**Interaction**: F (2, 72) = 0,9436; P = 0,3940 **Sex**: F (1, 72) = 4,565; P = 0,0360 **Treatment** F (2, 72) = 0,6104; P = 0,5459	**FEMALE** "Sham vs. CBD" P = 0,2198 "Sham vs. THC" P = 0,9226 "CBD vs. THC" P = 0,3530 **MALE** "Sham vs. CBD" P = 0,9470 "Sham vs. THC" P = 0,8896 "CBD vs. THC" P = 0,9937 **FEMALE vs. MALE** "Sham" P = 0.0373 "CBD" P = 0.8903 "THC" P = 0.1271
		CBD FEMALE	0.2	1.4	0	12		
		THC FEMALE	0.2	0.7	0	16		
		SHAM MALE	0.3	1.1	0	11		
		CBD MALE	0.2	1.8	0.02	10		
		THC MALE	0.2	0.9	0	16		
	Open arms	SHAM FEMALE	0	0.08	0	13	**Interaction**: F (2, 68) = 0,1873; P = 0,8297 **Sex**: F (1, 68) = 27,85; P < 0,0001 **Treatment** F (2, 68) = 4,092; P = 0,0210	**FEMALE** "Sham vs. CBD" P = 0,5994 "Sham vs. THC" P = 0,2458 "CBD vs. THC" P = 0,8614 **MALE** "Sham vs. CBD" P = 0,2025 "Sham vs. THC" P = 0,0530 "CBD vs. THC" P = 0,9023 **FEMALE vs. MALE** "Sham" P = 0.0170 "CBD" P = 0.0030 "THC" P = 0.0003
		CBD FEMALE	0.026	0.3	0	12		
		THC FEMALE	0.08	0.3	0	16		
		SHAM MALE	0.1	0.4	0	11		
		CBD MALE	0.2	0.5	0.08	10		
		THC MALE	0.3	0.7	0	16		
	Closed arms	SHAM FEMALE	8.4	22.6	3.7	13	**Interaction**: F (2, 72) = 0,7192; P = 0,4906 **Sex**:F (1, 72) = 0,8793; P = 0,3515 **Treatment** F (2, 72) = 19,79; P < 0,0001	**FEMALE** "Sham vs. CBD" P = 0,0008 "Sham vs. THC" P = 0,2116 "CBD vs. THC" P = 0,0581 **MALE**
		CBD FEMALE	2.7	9.5	1.4	12		

	THC FEMALE	5.3	14.2	2.6	16	"Sham vs. CBD" P < 0,0001 "Sham vs. THC" P = 0,1856 "CBD vs. THC" P = 0,0015 **FEMALE vs. MALE** "Sham" P = 0,2779 "CBD" P = 0,6598 "THC" P = 0,2756
	SHAM MALE	11.2	20.3	4.8	11	
	CBD MALE	2.1	5.3	1.1	10	
	THC MALE	8.5	20.2	3.7	16	

Prenatal cannabinoids induce a universal increase in repetitive defensive behavior.

The Marble Burying (MB) task was employed as an ethological measure of defensive persistence, where the burying of non-reactive objects serves as a proxy for repetitive, stereotyped behaviors responding to potential environmental threats (33, 34). This assay provides a distinct dimension of emotional reactivity that complements the EPM by probing behavioral persistence and compulsivity.

We previously reported that prenatal CBD exposure increases marble burying in both male and female offspring (18); however, the long-term impact of prenatal THC on this specific phenotype remained uncharacterized. To address this, we applied our established exposure protocol to the current cohort. Analysis revealed that offspring exposed to either CBD or THC buried significantly more marbles than Sham controls (Fig. 2, Table 5). This increase was observed in both males and females, identifying dysregulation of pre-existing motor loops as a universal endophenotype of prenatal cannabinoid exposure. In contrast, Sham progeny exhibited comparable baseline burying levels across sexes, indicating no innate sex differences in this measure.

Table 5
Analysis of MB. Statistical significance defined as p-value < 0.05.

Measurement	Treatment	Median	Max	Min	N	*Two-way ANOVA Main effects and interactions*	*Multiple comparison (Šidák's post hoc test)*
Buried marbles	SHAM FEMALE	13	17	4	28	**Interaction**: F (2, 127) = 0,03546; P = 0,9652 **Sex**: F (1, 127) = 5,234; P = 0,0238 **Treatment** F (2, 127) = 28,35; P < 0,0001	**FEMALE** "Sham vs. CBD" P < 0.0001 "Sham vs. THC" P = 0,0033 "CBD vs. THC" P = 0,5010 **MALE** "Sham vs. CBD" P < 0,0001 "Sham vs. THC" P = 0,0050 "CBD vs. THC" P = 0,6992 **FEMALE vs. MALE** "Sham" P = 0,0927 "CBD" P = 0,2262 "THC" P = 0,2448
	CBD FEMALE	17	18	12	25		
	THC FEMALE	15	18	11	15		
	SHAM MALE	13.5	18	8	28		
	CBD MALE	17	19	12	23		
	THC MALE	17	19	8	14		

From executive failure to circuit remodeling.

The concomitant manifestation of motor stereotypies and increased risk appraisal signifies a fundamental disruption of cognitive arbitration, the executive computation required to resolve environmental uncertainty and orchestrate adaptive behavioral transitions (33, 34). Given the central role of the medial prefrontal cortex (mPFC) in the top-down gating of defensive strategies (35–37), we reasoned that the observed behavioral inflexibility reflects a pathological remodeling of prefrontal efferent circuitry. To isolate the cellular determinants of this executive failure, we interrogated the functional integrity of Layer-5 (L5) pyramidal neurons, the principal projection node of the mPFC (38–40). We specifically tested whether the loss of behavioral flexibility is grounded in a collapse of synaptic adaptability and circuit-level excitability, evaluating the degree to which an endophenotype of synaptic rigidity restricts the capacity for context-dependent behavioral modulation.

Prenatal cannabinoids differentially reshape the intrinsic excitability of mPFC projection neurons.

To determine how gestational cannabinoid exposure influences the fundamental biophysical properties of mPFC output neurons, we interrogated the passive membrane characteristics of Layer 5 (L5) pyramidal neurons in adult offspring (9) (Supplementary Fig. 2, Table 6). Our results indicate that THC and CBD reorganize neuronal membrane properties through distinct, sex-dependent mechanisms.

Table 6
Active and passive membrane properties of mPFC layer V pyramidal neurons. Statistical significance defined as p-value < 0.05.

Measure	Treatment	Median	Max	Min	n/N	*Two-way ANOVA Main effects and interactions*	*Multiple comparison (Šidák's post hoc test)*
Resting Membrane Potential (mV)	SHAM FEMALE	-69.96	-61.04	-78.74	34/9	**Interaction** F (2, 178) = 3,031 P = 0,0508 **Sex** F (1, 178) = 0,1751 P = 0,6761 **Treatment** F (2, 178) = 2,008 P = 0,1373	**FEMALE** "Sham vs. CBD" P = 0,2166 "Sham vs. THC" P = 0,3717 "CBD vs. THC" P = 0,9702 **MALE** "Sham vs. CBD" P = 0,9432 "Sham vs. THC" P = 0,0941 "CBD vs. THC" P = 0,0309 **FEMALE vs. MALE** "Sham" P = 0,1760 "CBD" P = 0.9301 "THC" P = 0.039
	CBD FEMALE	-73.52	-60.27	-85.39	31/10		
	THC FEMALE	-72.75	-63.74	-80.74	26/9		
	SHAM MALE	-73.01	-64.13	-83.08	27/8		
	CBD MALE	-73.78	-58.33	-84.03	34/14		
	THC MALE	-70.41	-57.31	-81.01	30/8		
Rheobase (pA)	SHAM FEMALE	70	140	20	34/9	**Interaction** F (2, 175) = 1,407 P = 0,2477 **Sex** F (1, 175) = 0,3864 P = 0,5350 **Treatment** F (2, 175) = 9,386 P = 0,0001	**FEMALE** "Sham vs. CBD" P = 0,5066 "Sham vs. THC" P = 0,0003 "CBD vs. THC" P = 0,0157 **MALE** "Sham vs. CBD" P = 0,2259 "Sham vs. THC" P = 0,0763 "CBD vs. THC" P = 0,8133 **FEMALE vs. MALE** "Sham" P = 0,9764 "CBD" P = 0.5369 "THC" P = 0.1014
	CBD FEMALE	70	170	10	30/10		
	THC FEMALE	110	210	40	26/9		
	SHAM MALE	60	170	30	27/8		
	CBD MALE	80	160	20	34/14		
	THC MALE	90	230	20	30/8		
Capacitance (pF)	SHAM FEMALE	126.38	243.34	64.22	35/9	**Interaction** F (2, 165) = 2,429 P = 0,0912 **Sex** F (1, 165) = 1,824 P = 0,1787 **Treatment** F (2, 165) = 1,970 P = 0,1428	**FEMALE** "Sham vs. CBD" P = 0,9555 "Sham vs. THC" P = 0,1038 "CBD vs. THC" P = 0,0673 **MALE**
	CBD FEMALE	136.41	259.52	45.07	30/10		

	THC FEMALE	106.72	176.69	29.94	22/9		"Sham vs. CBD" P = 0,2672 "Sham vs. THC" P = 0,7178
	SHAM MALE	131.62	210.33	61.83	24/8		"CBD vs. THC" P = 0,7218 **FEMALE vs.MALE**
	CBD MALE	102.99	222.68	35.81	33/14		"Sham" P = 0,5480 "CBD" P = 0,0110
	THC MALE	106.63	180.86	40.08	27/8		"THC" P = 0,5313
Threshold (mV)	SHAM FEMALE	-41.14	-31.95	-48.50	34/9	**Interaction** F (2, 176) = 0,9864 P = 0,3750 **Sex** F (1, 176) = 0,01012 P = 0,9200 **Treatment** F (2, 176) = 2,382 P = 0,0953	**FEMALE** "Sham vs. CBD" P = 0,8112
	CBD FEMALE	-39.92	-32.53	-53.62	31/10		"Sham vs. THC" P = 0,2421 "CBD vs. THC" P = 0,0815 **MALE**
	THC FEMALE	-42.40	-29.88	-50.00	26/9		"Sham vs. CBD" P = 0,6621 "Sham vs. THC" P = 0,4598
	SHAM MALE	-39.95	-34.73	-48.18	27/8		"CBD vs. THC" P = 0,9273 **FEMALE vs. MALE**
	CBD MALE	-41.03	-36.96	-47.87	34/14		"Sham" P = 0,6825 "CBD" P = 0.2769
	THC MALE	-42.44	-35.46	-48.98	30/8		"THC" P = 0.43339
Number of APs (+ 400pA)	SHAM FEMALE	17	23	9	33/9	**Interaction** F (2, 178) = 3,031 P = 0,0508 **Sex** F (1, 178) = 0,1751 P = 0,6761 **Treatment** F (2, 178) = 2,008 P = 0,1373	**FEMALE** "Sham vs. CBD" P = 0,2166
	CBD FEMALE	17	29	11	31/10		"Sham vs. THC" P = 0,3717 "CBD vs. THC" P = 0,9702 MALE
	THC FEMALE	17	27	9	26/9		"Sham vs. CBD" P = 0,9432 "Sham vs. THC" P = 0,0941
	SHAM MALE	17	31	11	27/8		"CBD vs. THC" P = 0,0309 **FEMALE vs. MALE**
	CBD MALE	18.5	35	7	34/14		"Sham" P = 0,1760
	THC MALE	21	50	9	30/8		"CBD" P = 0.9301 "THC" P = 0.039

Table 7
Voltage membrane response per current steps in mPFC pyramidal neurons in both sexes and treatment. Statistical significance defined as p-value < 0.05.

Measure	Injected Current (pA)	Female Sham			Female CBD			*corrected p-value* *Multiple Mann-Whitney test*	Female THC			*corrected p-value* *Multiple Mann-Whitney test*
		Mean	SEM	n/N	Mean	SEM	n/N		Mean	SEM	n/N	
Voltage changes per current step (ΔVm)	*-400*	-39.13	1.66	33/9	-39.84	2.18	31/10	> 0.99	-33.44	1.95	26/9	0.24
	-350	-35.88	1.55		-36.41	1.98		> 0.99	-30.53	1.81		0.24
	-300	-32.27	1.42		-32.81	1.81		> 0.99	-27.26	1.64		0.24
	-250	-28.72	1.33		-28.99	1.64		> 0.99	-23.92	1.50		0.21
	-200	-24.84	1.21		-25.02	1.49		> 0.99	-20.22	1.34		0.17
	-150	-20.44	1.09		-20.67	1.34		> 0.99	-16.31	1.15		0.17
	-100	-15.07	0.87		-15.34	1.10		> 0.99	-11.70	0.88		0.12
	-50	-8.52	0.54		-8.71	0.73		> 0.99	-6.38	0.55		0.11
	0	-0.02	0.07		0.01	0.07		1.0	0.04	0.06		0.55
	50	11.61	1.03		10.65	1.00		1.0	8.23	0.90		0.17
	100	19.61	1.22		20.66	1.77		> 0.99	15.81	1.41		0.24
	150	24.51	1.26		26.20	1.68		1.0	22.49	1.91		0.55
	200	31.96	1.85		31.50	1.92		> 0.99	29.07	2.31		0.55
	Injected Current (pA)	**Male Sham**			**Male CBD**			**corrected p-value** **Multiple Mann-Whitney test**	**Male THC**			**corrected p-value** **Multiple Mann-Whitney test**
		Mean	SEM	n/N	Mean	SEM	n/N		Mean	SEM	n/N	
Voltage changes per current step (ΔVm)	*-400*	-46.43	20.91	27/8	-38.23	11.54	34/14	0.64	-45.41	16.66	30/8	1.00
	-350	-42.01	17.90		-34.58	9.75		0.64	-41.05	14.28		1.00
	-300	-37.69	15.08		-31.05	8.72		0.64	-36.65	12.47		1.00
	-250	-32.86	12.90		-27.31	7.73		0.64	-31.89	10.63		1.00
	-200	-28.27	11.09		-23.48	6.94		0.64	-26.99	8.93		1.00
	-150	-23.42	9.16		-19.25	6.00		0.64	-21.47	7.23		0.99
	-100	-17.47	7.28		-14.25	4.75		0.64	-15.48	5.51		0.98
	-50	-10.04	4.39		-7.89	3.10		0.64	-8.52	3.17		0.91
	0	0.15	0.43		0.07	0.53		0.77	-0.05	0.44		0.83
	50	12.86	6.53		10.49	4.26		0.74	9.53	3.33		0.45
	100	22.12	9.56		20.46	8.60		0.77	16.69	5.92		0.08
	150	26.87	7.97		26.15	6.81		0.77	23.01	8.55		0.31
	200	32.32	8.79		30.97	8.60		0.75	24.82	6.98		0.01

Across both sexes, prenatal exposure to either CBD or THC did not alter the resting membrane potential (RMP), indicating a preservation of the tonic membrane state (Supplementary Fig. 2B). However, intrinsic excitability was selectively modulated in female offspring: THC exposure, but not CBD, uniquely elevated the rheobase, signifying that a higher depolarizing current is required to reach the firing threshold in these neurons (Supplementary Fig. 2C). Notably, rheobase values in males remained unaffected by either treatment (Supplementary Fig. 2C, Table 6). Furthermore, membrane capacitance and the steady-state current-voltage (I-V) relationship remained stable across all treatment groups (Supplementary Fig. 2D-F, Table 6). Collectively, these findings suggest that gestational cannabinoid exposure causes targeted remodeling of specific excitability parameters rather than a global disruption of the core resistive or capacitive properties of the somatic membrane.

Prenatal THC augments the repetitive firing capacity of male mPFC projection neurons

To evaluate active firing dynamics, we characterized the relationship between input current and spike frequency (IV curve) in adult L5 pyramidal neurons (Fig. 3, Table 8). These analyses revealed a sex-specific vulnerability to prenatal THC exposure, with alterations in mPFC excitability confined exclusively to male offspring, a finding consistent with our previous observations in rats (9). In females, L5 pyramidal neurons displayed stable intrinsic excitability and conserved firing rates across all treatment conditions (Fig. 3A).

Table 8
Voltage membrane response per current steps in mPFC pyramidal neurons in both sexes and treatment. Statistical significance defined as p-value < 0.05.

Measure	Injected Current (pA)	Female Sham			Female CBD			*corrected p-value*	Female THC			*corrected p-value*
		Mean	SEM	n/N	Mean	SEM	n/N	*Multiple Mann-Whitney test*	Mean	SEM	n/N	*Multiple Mann-Whitney test*
Number of action potentials	0	0.00	0.00	33/9	0.00	0.00	31/10	> 0.99	0.00	0.00	26/9	> 0.99
	50	0.55	1.30		0.56	1.37		0.86	0.23	0.82		0.46
	100	3.67	2.68		2.82	3.31		0.85	2.04	2.71		0.14
	150	7.33	3.31		6.29	4.46		0.85	4.96	4.42		0.14
	200	10.48	3.47		9.65	4.95		0.85	8.19	5.48		0.33
	250	12.85	3.44		12.47	4.97		0.85	11.27	5.77		0.56
	300	14.76	3.15		14.79	5.01		0.86	13.62	5.80		0.69
	350	16.15	3.01		16.41	4.90		0.86	16.08	5.15		0.99
	400	16.85	3.29		17.47	4.80		> 0.99	17.50	5.05		0.99
	450	17.21	4.18		18.32	4.75		0.86	18.85	5.39		0.56
	500	17.33	5.11		18.85	5.02		0.86	19.96	6.23		0.32
	550	17.09	6.18		19.00	5.75		0.86	20.73	6.48		0.14
	600	16.76	7.07		19.38	6.45		0.85	20.85	7.44		0.16
	Injected Current (pA)	**Male Sham**			**Male CBD**			**corrected p-value**	**Male THC**			**corrected p-value**
		Mean	SEM	n/N	Mean	SEM	n/N	**Multiple Mann-Whitney test**	Mean	SEM	n/N	**Multiple Mann-Whitney test**
Number of action potentials	0	0.00	0.00	27/8	0	0	34/14	> 0.99	0.00	0.00	30/8	> 0.999999
	50	0.88	0.30		0.67	0.273		0.89	0.63	0.26		0.89
	100	3.56	0.60		3.5	0.618		0.89	3.60	0.72		0.91
	150	6.80	0.72		7	0.839		> 0.99	7.97	1.09		0.97
	200	10.04	0.74		10.64	0.867		> 0.99	12.13	1.40		0.89
	250	12.88	0.70		13.73	0.866		> 0.99	16.30	1.58		0.66
	300	14.96	0.67		16.17	0.88		0.89	19.73	1.71		0.16
	350	16.56	0.70		17.91	0.906		0.89	22.53	1.83		0.03
	400	17.88	0.76		19.11	0.99		0.89	24.37	1.77		0.01
	450	18.52	0.95		19.76	0.954		0.89	24.90	1.53		0.01
	500	18.56	1.21		20.08	1.048		0.89	25.03	1.60		0.02
	550	19.04	1.50		20.73	1.161		0.89	25.07	1.76		0.08
	600	19.16	1.64		20.94	1.291		0.89	25.50	1.97		0.08

In contrast, THC-exposed males exhibited a marked potentiation of intrinsic excitability, characterized by an elevated spike frequency in response to depolarizing current injections. This gain in firing capacity was particularly pronounced at higher stimulus intensities

(Fig. 3B–D). Importantly, this hyperexcitability occurred independently of changes in the voltage-dependent threshold for spike initiation, as action potential (AP) thresholds remained unchanged across both sex and treatment groups (Fig. 3C). Together, these results suggest that prenatal THC exposure induces a persistent recalibration of the intrinsic excitability in the male mPFC without altering the fundamental gate of spike generation.

Prenatal cannabinoids drive sex-divergent rescaling of excitatory drive and synaptic kinetics.

To determine whether the observed modifications in intrinsic excitability were coupled with altered synaptic input, we interrogated spontaneous excitatory postsynaptic currents (sEPSCs) in L5 pyramidal neurons (Fig. 4, Table 9). These measurements revealed a sex-dependent reorganization of the excitatory landscape following gestational cannabinoid exposure.

Table 9
Characterization of excitatory postsynaptic currents features recorded in layer V pyramidal neurons. Statistical significance defined as p-value < 0.05.

Measure	Sex	Treatment	Median	MAX	MIN	n/N	*Two-way ANOVA Main effects and interactions*	*Multiple comparison (Šidák's post hoc test)*
sEPSCs Amplitude (pA)	Female	Sham	13.94	23.13	10.31	24//9	**Interaction** F (2, 178) = 3,031 P = 0,0508 **Sex** F (1, 178) = 0,1751 P = 0,6761 **Treatment** F (2, 178) = 2,008 P = 0,1373	**FEMALE** "Sham vs. CBD" P = 0,0338 "Sham vs. THC" P = 0,0596 "CBD vs. THC" P = 0,9945 **MALE** "Sham vs. CBD" P = 0,5135 "Sham vs. THC" P = 0,1286 "CBD vs. THC" P = 0,7157 **FEMALE vs. MALE** "Sham" P = 0,0962 "CBD" P = 0,0594 "THC" P = 0,0105
		CBD	16.47	23.99	9.03	26//12		
		THC	16.01	25.00	10.58	21//9		
	Male	Sham	16.13	23.57	10.60	21//8		
		CBD	13.63	23.86	10.52	21//13		
		THC	13.10	20.30	10.55	27//8		
sEPSCs Frequency (Hz)	Female	Sham	2.64	6.52	1.23	24//9	**Interaction** F (2, 133) = 0,1497 P = 0,8611 **Sex** F (1, 133) = 0,6387 P = 0,4256 **Treatment** F (2, 133) = 11,17 P < 0,0001	**FEMALE** "Sham vs. CBD" P = 0,0226 "Sham vs. THC" P = 0,7347 "CBD vs. THC" P = 0,0030 **MALE** "Sham vs. CBD" P = 0,2004 "Sham vs. THC" P = 0,3718 "CBD vs. THC" P = 0,0046 **FEMALE vs. MALE** "Sham" P = 0,9857 "CBD" P = 0,4446 "THC" P = 0,5394
		CBD	4.16	7.49	1.17	26//12		
		THC	2.79	6.16	0.40	21//9		
	Male	Sham	2.79	5.38	1.11	21//8		
		CBD	3.74	6.08	2.07	21//13		
		THC	2.24	6.17	0.52	27//8		
Rise time (ms)	Female	Sham	0.99	1.53	0.55	24//9	**Interaction** F (2, 134) = 0,06577 P = 0,9364 **Sex** F (1, 134) = 0,1151 P = 0,7349 **Treatment** F (2, 134) = 50,47 P < 0,0001	**FEMALE** "Sham vs. CBD" P = 0,2539 "Sham vs. THC" P = < 0,0001 "CBD vs. THC" P = < 0,0001 **MALE** "Sham vs. CBD" P = 0,2956 "Sham vs. THC" P = < 0,0001 "CBD vs. THC" P = < 0,0001 **FEMALE vs. MALE** "Sham" P = 0,7517 "CBD" P = 0,7161 "THC" P = 0,9217
		CBD	0.93	1.46	0.63	26//12		
		THC	0.62	1.02	0.45	21//9		
	Male	Sham	1.02	1.39	0.69	21//8		
		CBD	0.87	1.41	0.64	21//13		
		THC	0.67	0.84	0.43	27//8		

Decay time (ms)	Female	Sham	6.32	10.85	4.03	24//9	**Interaction** F (2, 134) = 1,447 P = 0,2390 **Sex** F (1, 134) = 1,087 P = 0,2990 **Treatment** F (2, 134) = 1,511 P = 0,2244	**FEMALE** "Sham vs. CBD" P = 0,0887 "Sham vs. THC" P = 0,2037 "CBD vs. THC" P = 0,9503 **MALE** "Sham vs. CBD" P = 0,9136 "Sham vs. THC" P = 0,8032 "CBD vs. THC" P = 0,5401 **FEMALE vs. MALE** "Sham" P = 0,4761 "CBD" P = 0,3718 "THC" P = 0,0998
		CBD	5.73	10.73	3.95	26//12		
		THC	5.82	8.77	4.18	21//9		
	Male	Sham	6.40	9.41	3.76	21//8		
		CBD	6.75	12.00	2.95	21//13		
		THC	7.01	9.12	4.11	27//8		

In female offspring, prenatal CBD exposure induced a robust augmentation of excitatory drive, characterized by significant increases in both mean sEPSC amplitude (Supplementary Fig. 3A) and event frequency (Supplementary Fig. 3B). Log-normal distributional analysis unmasked a categorical rightward shift in event magnitude, indicating a greater proportion of high-amplitude synaptic entries in CBD-treated females (Fig. 4C). This was paralleled by a significant shortening of inter-event intervals (Fig. 4E), confirming a sustained elevation in the rate of glutamate release. While THC-exposed females similarly exhibited a shift toward larger-amplitude events (Fig. 4C), this did not translate into an increase in mean sEPSC amplitude or frequency (Fig. 4E, Supplementary Fig. 3A-B), suggesting a more restricted remodeling of the synaptic pool.

Male offspring displayed a distinct, non-canonical synaptic phenotype. In CBD-exposed males, distributional analysis revealed an increased proportion of small-amplitude sEPSCs (Fig. 4E) and a subset of neurons with shortened inter-event intervals (Fig. 4F); however, these stochastic shifts were insufficient to alter global mean event amplitude or frequency (Supplementary Fig. 3A-B).

Beyond magnitude and frequency, the temporal architecture of synaptic signaling dictates the precision of dendritic integration. We observed that gestational cannabinoids fundamentally reshaped receptor-mediated timing (Fig. 4H-I, Table 9). Specifically, prenatal THC exposure—across both sexes—accelerated sEPSC rise-time kinetics (Fig. 4H), while decay times remained stable (Fig. 4I). This abbreviation of the rising phase is highly consistent with a discrete remodeling of the synaptic microarchitecture, potentially reflecting a shift in AMPA receptor subunit stoichiometry toward faster-activating configurations or a selective redistribution of excitatory inputs toward more proximal dendritic compartments.

Prenatal Cannabinoids Drive Sex-Specific Remodeling of the Inhibitory Landscape and Temporal Tuning

To determine if the GABAergic inhibitory drive within the mPFC microcircuitry underwent a concomitant reorganization, we interrogated spontaneous inhibitory postsynaptic currents (sIPSCs) in adult L5 pyramidal neurons (Fig. 5, Table 10).

Table 10
Characterization of inhibitory postsynaptic currents features recorded in layer V pyramidal neurons. Statistical significance defined as p-value < 0.05.

Measure	Sex	Treatment	Median	MAX	MIN	n/N	*Two-way ANOVA Main effects and interactions*	*Multiple comparison (Šidák's post hoc test)*
sIPSCs Amplitude (pA)	Female	Sham	33.62	70.74	21.87	20//6	**Interaction** F (2, 133) = 2,858 P = 0,0609 **Sex** F (1, 133) = 1,456 P = 0,2297 **Treatment** F (2, 133) = 8,210 P = 0,0004	**FEMALE** "Sham vs. CBD" P = 0,0219 "Sham vs. THC" P = 0,9911 "CBD vs. THC" P = 0,0150 **MALE** "Sham vs. CBD" P = 0,9796 "Sham vs. THC" P = 0,0037 "CBD vs. THC" P = 0,0122 **FEMALE vs. MALE** "Sham" P = 0,0089 "CBD" P = 0,8213 "THC" P = 0,7457
		CBD	55.64	86.65	14.58	27//7		
		THC	36.46	76.54	18.34	21//5		
	Male	Sham	51.75	75.86	29.07	27//7		
		CBD	48.26	105.22	10.33	21//7		
		THC	36.51	56.71	15.67	24//5		
sIPSCs Frequency (Hz)	Female	Sham	5.31	8.66	0.35	20//6	**Interaction** F (2, 133) = 0,3607 P = 0,6979 **Sex** F (1, 133) = 3,416 P = 0,0668 **Treatment** F (2, 133) = 4,351 P = 0,0148	**FEMALE** "Sham vs. CBD" P = 0,3179 "Sham vs. THC" P = 0,4901 "CBD vs. THC" P = 0,0227 **MALE** "Sham vs. CBD" P = 0,8261 "Sham vs. THC" P = 0,5837 "CBD vs. THC" P = 0,2922 **FEMALE vs. MALE** "Sham" P = 0,2071 "CBD" P = 0,6873 "THC" P = 0,1335
		CBD	5.63	13.24	0.66	27//7		
		THC	4.01	8.76	1.02	21//5		
	Male	Sham	6.12	9.41	0.73	27//7		
		CBD	6.84	11.07	1.52	21//7		
		THC	4.95	10.34	1.59	24//5		
Rise time (ms)	Female	Sham	0.59	0.95	0.34	20//6	**Interaction** F (2, 132) = 7,901 P = 0,0006 **Sex** F (1, 132) = 2,956 P = 0,0879 **Treatment** F (2, 132) = 2,282 P = 0,1061	**FEMALE** "Sham vs. CBD" P = 0,0102 "Sham vs. THC" P = 0,0281 "CBD vs. THC" P = 0,9834 **MALE** "Sham vs. CBD" P = 0,9120 "Sham vs. THC" P = 0,0086 "CBD vs. THC" P = 0,0404 **FEMALE vs. MALE** "Sham" P = 0,0001 "CBD" P = 0,5114 "THC" P = 0,1072
		CBD	0.46	0.80	0.36	27//7		
		THC	0.52	0.78	0.26	21//5		
	Male	Sham	0.45	0.61	0.37	27//7		
		CBD	0.45	0.75	0.35	21//7		
		THC	0.54	0.90	0.38	24//5		

Decay time (ms)	Female	Sham	7.93	12.75	6.08	20//6	**Interaction** F (2, 127) = 2,480 P = 0,0878 **Sex** F (1, 127) = 5,846 P = 0,0170 **Treatment** F (2, 127) = 9,965 P < 0,0001	**FEMALE** "Sham vs. CBD" P = 0,0228 "Sham vs. THC" P = 0,7587 "CBD vs. THC" P = 0,0013 **MALE** "Sham vs. CBD" P = 0,9496 "Sham vs. THC" P = 0,0052 "CBD vs. THC" P = 0,0210 **FEMALE vs. MALE** "Sham" P = 0,0024 "CBD" P = 0,9041 "THC" P = 0,3689
		CBD	6.81	11.29	3.52	27//7		
		THC	8.49	14.56	3.45	21//5		
	Male	Sham	6.63	11.42	4.45	27//7		
		CBD	6.65	10.74	4.13	21//7		
		THC	8.45	10.12	5.67	24//5		

Consistent with the excitatory findings, CBD-exposed females exhibited a robust gain in inhibitory transmission. This was evidenced by increased sIPSCs mean amplitudes (Supplementary Fig. 4A) and a significant enrichment of large-amplitude inhibitory events (Fig. 5C), while sIPSCs frequency remained stable (Fig. 5E, Supplementary Fig. 4B). Conversely, THC-exposed females displayed an attenuated inhibitory profile; although sIPSCs frequency was conserved on average, distributional analysis revealed an increased proportion of longer inter-event intervals, suggesting a reduction in the probability of GABA-A receptor activation (Fig. 5E-F).

In male offspring, cannabinoid exposure resulted in a generalized weakening of inhibitory synaptic strength. THC-exposed males exhibited significantly decreased mean amplitudes (Supplementary Fig. 4A), and both THC and CBD exposure induced a categorical shift toward smaller-amplitude sIPSCs (Fig. 5D). Like the female cohort, sIPSCs average frequency was unaffected across male treatment groups (Supplementary Fig. 4B). Together, these data uncover a sexually divergent inhibitory signature: female CBD exposure induces an overall potentiation of inhibitory throughput, while prenatal THC (in both sexes) and male CBD exposure lead to an attenuation of the total inhibitory synaptic drive.

Beyond synaptic magnitude, the temporal precision of inhibition was differentially modulated. In females, both THC and CBD exposure accelerated sIPSCs rise times (Fig. 5H). However, their effects on decay kinetics diverged sharply: CBD exposure accelerated decay, while THC significantly prolonged inhibitory decay (Fig. 5I). In males, CBD had no discernable effect on kinetics, whereas THC exposure generally slowed inhibitory signaling, characterized by increased rise and decay times (Fig. 5H-I). Collectively, these findings indicate that the temporal "tuning" of inhibitory transmission is uniquely sensitive to the specific cannabinoid and the sex of the offspring, adding a layer of biophysical complexity to the circuit-wide synaptic reorganization.

Prenatal cannabinoids drive sex-specific homeostatic vs. pathological rescaling of the mPFC E/I landscape.

To characterize the integrated functional impact of prenatal cannabinoid exposure on mPFC synaptic processing, we quantified the net excitatory-inhibitory (E/I) balance in adult L5 pyramidal neurons (Fig. 6, Table 11). By analyzing the cumulative probability distributions of total synaptic charge transfer, we integrated the previously observed changes in amplitude and frequency into a single measure of synaptic throughput.

Table 11
Comparison of cumulative distributions of excitatory/inhibitory total charge transferred by postsynaptic currents recorded in layer V pyramidal neurons. Statistical significance defined as p-value < 0.05.

Measure	Sex	Treatment	Median	MAX	MIN	n/N	*Kolmogorov-Smirnov D*	*Kolmogorov-Smirnov test (p-value)*
Total excitatory charge transferred (-pC)	Female	Sham	81.24	300.00	46.70	24//9		
		CBD	129.40	402.10	34.22	26//12	0.555	0.001
		THC	93.66	323.80	12.34	21//9	0.238	0.549
	Male	Sham	81.49	376.80	14.82	21//8		
		CBD	102.40	339.50	44.32	21//13	0.297	0.301
		THC	79.38	296.60	8.40	27//8	0.201	0.726
Total inhibitory charge transferred (-pC)	Female	Sham	458.00	1005.00	65.73	20//6		
		CBD	570.20	1755.00	33.71	27//7	0.357	0.106
		THC	274.80	917.50	56.35	21//5	0.462	0.025
	Male	Sham	640.90	1387.00	55.48	27//7		
		CBD	683.00	1561.00	81.56	21//7	0.164	0.908
		THC	413.70	1246.00	114.40	24//5	0.384	0.047

In female offspring, the data unmasked a compound-specific reorganization of the synaptic landscape. Prenatal CBD exposure induced a robust rightward shift in the cumulative distribution of excitatory charge transfer (Fig. 6A; D = 0.555, p = 0.001), which was accompanied by a reciprocal, though non-significant, rightward trend in inhibitory charge (Fig. 6B; D = 0.357, p = 0.106). This pattern suggests a homeostatic rescaling of the female mPFC, where the augmentation of excitatory drive is partially countered by a parallel enhancement of inhibitory input. In stark contrast, prenatal THC exposure favored a pro-excitatory shift; a modest qualitative increase in excitation (Fig. 6A) was coupled with a significant leftward collapse of inhibitory charge transfer (Fig. 6B; D = 0.462, p = 0.025).

Male offspring exhibited a distinct profile of synaptic resilience. In the CBD lineage, both excitatory and inhibitory charge distributions remained stable relative to Sham controls (Fig. 6E-F). While THC-exposed males displayed a modest leftward shift in inhibitory charge transfer (D = 0.384, p = 0.047), excitatory drive remained unaffected, suggesting a more limited remodeling of the male synaptic pool.

To statistically evaluate these shifts, we utilized a bootstrap-based estimation of the E/(E + I) index (see Methods). Statistical significance was defined by the consistency of Delta E/I values, with contrasts considered significant when more than 95% of bootstrap samples fell on the same side of the zero-null (Fig. 6D, G-H). This analysis revealed that THC-exposed females exhibit a significantly elevated E/I index compared to Sham controls, representing a fundamental loss of inhibitory governance. Conversely, CBD-exposed females maintained a stable net E/I balance, as the potentiation of excitatory drive was effectively offset by the parallel increase in inhibitory throughput (Fig. 6C). In males, neither THC nor CBD exposure produced significant perturbations of the E/I index, reflecting a relative conservation of net synaptic balance despite the underlying shifts in inhibitory charge.

Collectively, these findings demonstrate that gestational cannabinoids reshape the mPFC synaptic landscape through sex- and compound-specific trajectories: while females undergo a significant pro-excitatory reorganization, most notably after THC exposure, males preserve a stable net E/I ratio.

Prenatal CBD and THC exposure converge to abrogate eCB-LTD in the adult mPFC

To evaluate how gestational cannabinoid exposure impacts synaptic flexibility, we interrogated endocannabinoid-mediated long-term depression (eCB-LTD), a hallmark of mPFC plasticity that we previously identified as vulnerable to prenatal THC in rats (9, 12). In Sham-exposed offspring of both sexes, low-frequency stimulation (10 Hz, 10 min) reliably induced robust eCB-LTD, characterized by a sustained reduction in fEPSP amplitude relative to baseline (Fig. 7A-D). Notably, this form of plasticity was completely absent in adult mice prenatally exposed to either CBD or THC. In both females (Fig. 7A-B) and males (Fig. 7C-D), fEPSP amplitudes failed to undergo depression following induction, remaining at or above baseline levels throughout the duration of the recording.

This global loss of eCB-LTD in THC-exposed female mice represents a significant divergence from our previous findings in rats, where this form of plasticity was selectively preserved in females (9). In the mouse model, however, prenatal exposure to either cannabinoid resulted in an equivalent functional outcome (Fig. 7E-F). CBD was as effective as THC in nullifying eCB-LTD, demonstrating that CBD does not confer protection against this specific synaptic disruption. Collectively, these data indicate that both cannabinoids converge on a shared pathological endpoint in the mouse mPFC: the absolute loss of activity-dependent synaptic depression across both sexes.

Prenatal CBD exposure selectively compromises LTP in the male mPFC

To determine if the identified deficits in synaptic flexibility extended to excitatory potentiation, we utilized theta-burst stimulation (TBS) to induce long-term potentiation (LTP). LTP serves as a primary mechanism for synaptic strengthening and is a hallmark of prefrontal function frequently disrupted in neuropsychiatric models (21, 41–43). TBS reliably elicited LTP in Sham, CBD, and THC-exposed offspring of both sexes, with fEPSP amplitudes significantly elevated above baseline (Fig. 8).

In female offspring, neither prenatal CBD nor THC exposure altered the magnitude of LTP (Fig. 8A, B, E). In contrast, a sex-specific vulnerability was evident in males: CBD exposure—but not THC—led to a marked reduction in LTP amplitude compared to Sham controls (Fig. 8C, D, F). These data demonstrate that prenatal CBD restricts the dynamic range of excitatory strengthening in the male mPFC, whereas LTP mechanisms remain resilient to gestational THC interference in both sexes.

This developmental profile reveals a stark divergence in the plasticity signatures induced by prenatal CBD versus THC. While both compounds abolish eCB-LTD, only CBD exposure diminishes the capacity for LTP, specifically within the male lineage. Synthesizing these results with our eCB-LTD data suggests that prenatal CBD induces a more pervasive state of synaptic rigidity in males. By compromising the circuit's ability to bidirectionally regulate synaptic weights, impairing both strengthening and weakening mechanisms, CBD exposure renders the male mPFC functionally inflexible, whereas the impact of THC is selectively restricted to the loss of synaptic depression.

Sex-specific effects of gestational CBD on synaptic weighting and NMDAR Kinetics

The fact that prenatal THC exposure did not impair LTP in either sex suggests that the mechanisms supporting excitatory strengthening, including NMDAR activation and AMPAR recruitment, remained functionally intact. Consequently, we designed experiments specifically to isolate the cellular substrates of synaptic rigidity, which represents a CBD-male-specific endophenotype in this dataset.

The selective loss of LTP in CBD-exposed males suggested a fundamental disruption of glutamatergic signaling. To determine if this was secondary to broad deficits in axonal recruitment, we first analyzed input-output relationships in the mPFC. The stimulus-response curves and maximal fEPSP amplitudes remained indistinguishable from Sham controls in both females (Supplementary Fig. 5A) and males (Supplementary Fig. 5B). These results indicate that prenatal CBD does not broadly impair basal synaptic efficacy or axonal excitability.

At glutamatergic synapses, the ratio of AMPA to NMDA receptor-mediated currents (A/N ratio) serves as a critical index of synaptic weight. An elevated A/N ratio typically reflects an increase in the contribution of AMPA receptors to the postsynaptic response, which can limit further potentiation through functional occlusion. Consistent with our hypothesis of a ceiling effect in males, CBD-treated males exhibited a significant elevation in the A/N ratio compared to Sham counterparts (Fig. 9A-B). In contrast, no changes in synaptic weight were observed in female offspring.

To further resolve the underlying shifts in NMDAR-mediated signaling, we analyzed the kinetic profiles of isolated NMDA currents. In male offspring, gestational CBD significantly prolonged the rise time of NMDA currents (Fig. 9C). Because LTP induction requires a rapid, high-magnitude calcium influx, this kinetic slowdown likely impairs the ability of the receptor to generate the sharp activation necessary for synaptic strengthening. Conversely, CBD-exposed females exhibited a significant acceleration of NMDA decay kinetics (Fig. 9D), a change absent in males.

Collectively, these data suggest that the failure of LTP in the male mPFC results from a dual failure of synaptic function: a state of baseline functional saturation (elevated A/N ratio) coupled with a kinetic slowdown of NMDAR activation. This combination appears to lock the male synapse in a rigid state, rendering it both less responsive to glutamate and incapable of further potentiation.

Discussion

The data demonstrate that PCE fundamentally hijacks prefrontal neurodevelopment, culminating in adult executive dysfunction through sex-specific pathological rewiring. By integrating ethological behavioral analysis with circuit-level electrophysiology, we show that while THC and CBD converge on a universal loss of prefrontal eCB-LTD, they induce strikingly divergent synaptic endophenotypes. Our findings challenge the prevailing perception of CBD as a benign alternative to THC (14–18), revealing that gestational CBD exposure produces unique executive failures and a state of synaptic rigidity in the adult mPFC.

A central finding of this study is the dissociation between classical anxiety and high-level executive dysfunction. Neither prenatal THC nor CBD altered traditional spatiotemporal metrics in the EPM, such as open-arm exploration, consistent with previous reports (8, 9). Instead, the deficits were localized to the microstructure of risk assessment and behavioral switching. The concomitant manifestation of motor stereotypies (MB) and increased risk appraisal (SAP) signifies a disruption of cognitive arbitration—the executive computation required to resolve approach-avoidance conflicts and orchestrate adaptive transitions (33, 34, 44, 45). The increase in SAP observed uniquely in CBD-exposed females reflects a state of hyper-vigilance or assessment arrest. We hypothesize that this phenotype emerges from a failure of the PFC to effectively gate environmental information, thereby precluding the resolution of uncertainty (18, 46). This specificity underscores that PCE does not induce a generalized affective shift, but rather a targeted weakening of the prefrontal mechanisms governing behavioral strategy.

At the synaptic level, the primary point of convergence across both sexes and compounds was the complete ablation of eCB-LTD. This shared physiological deficit provides a direct cellular correlate to the universal increase in repetitive, perseverative behaviors (MB) observed in all exposed groups. As a critical top-down constituent, eCB-LTD represents a plausible mechanism for the deselection of obsolete behavioral motor loops; its loss may thus create a circuit-level environment where behavioral strategies become pathologically inflexible. This deficit, consistent with previous reports of impaired eCB-LTD in various neurodevelopmental models (22, 23, 42, 47, 48), establishes the loss of synaptic flexibility as a universal endophenotype of prenatal cannabinoid exposure, marking a permanent disruption in the maturation of endocannabinoid-dependent prefrontal plasticity (9, 12, 13).

The loss of eCB-LTD in THC-exposed female mice represents a significant divergence from our previous findings in rats, where this form of plasticity was selectively preserved in females (9). This discrepancy likely reflects species-specific ontogenetic windows in the maturation of the prefrontal endocannabinoid system. It is possible that the female mouse mPFC undergoes a more concentrated period of eCB-dependent circuit refinement during the GD5-18 window, rendering it more vulnerable to pharmacological interference than the female rat. Alternatively, these results may point toward divergent CB1R signaling architectures between species, where the female mouse lacks the homeostatic buffers that allow the female rat to maintain functional receptor coupling following chronic prenatal exposure.

While the loss of eCB-LTD appeared universal, the magnitude of plasticity failure diverged sharply in male offspring. Prenatal THC exposure did not impair LTP in either sex, suggesting that the mechanisms supporting excitatory strengthening, including NMDAR activation and AMPAR recruitment, remained functionally intact. However, we designed experiments to isolate the cause of synaptic rigidity, which is a CBD-male-specific endophenotype in this dataset. In males, exposure to CBD is associated with a state of synaptic rigidity, characterized by a bidirectional collapse of plasticity where both eCB-LTD and NMDA-dependent LTP were disrupted. Mechanistically, this rigidity may be underpinned by elevated AMPA/NMDA ratios and a significant slowdown in NMDAR activation kinetics, changes which represent a state of functional synaptic saturation.

This ceiling effect likely imposes a top-down lock on prefrontal function. Because L5 pyramidal neurons serve as the primary output node of the mPFC, the identified rigidity means that the brain's final executive commands are essentially fixed or inflexible before they even reach downstream targets such as the striatum or amygdala. This freezing of the prefrontal output circuit effectively precludes the synaptic plasticity necessary for executive flexibility. This male-specific vulnerability suggests a profound developmental sensitivity to CBD that parallels, and in certain parameters appears to exceed, the detrimental effects of THC.

In contrast to the inflexible male circuit, female offspring exhibited divergent reorganizations of E/I balance and synaptic throughput. In CBD-exposed females, our observations point toward a homeostatic scaled-up architecture, characterized by a coordinated amplification of both excitatory and inhibitory drive. While this scaling appears to preserve the net E/I balance, we hypothesize that it may significantly increase synaptic noise and alter subsequent circuit throughput. We propose that this high-noise/high-throughput state provides the cellular substrate for the unique SAP deficits seen in these females: the circuit is functionally unstable, leading to the hyper-vigilant, indecisive risk-appraisal strategy observed behaviorally. Conversely, THC exposure in females led to a collapse of the net E/I balance toward a pro-excitatory state, representing a true circuit disinhibition. The distinction between scaled-up noise in CBD females versus disinhibited hyperexcitability in THC females, reveals that the mPFC does not respond to prenatal cannabinoids through

a uniform mechanism. Instead, it undergoes a selective rewiring of intrinsic excitability and synaptic integration that depends critically on compound identity.

Collectively, these results carry significant translational implications, particularly in the context of increasing CBD consumption during pregnancy. Our data suggest that CBD may not represent a benign alternative to THC; rather, it appears to induce a discrete set of sex-specific molecular signatures. These include a state of synaptic rigidity in males and a putative noisy executive failure in females, highlighting the divergent ways in which prenatal cannabinoid exposure may disrupt prefrontal maturation. The sex-specificity of these effects underscores the urgent need for sex-disaggregated analyses in both preclinical and clinical cannabinoid research. In sum, prenatal cannabinoid exposure does not simply dampen or excite the developing cortex; it reprograms the fundamental rules of synaptic integration and plasticity. By identifying the divergence between universal hallmarks (eCB-LTD loss) and sex-specific trajectories, this study provides a biological framework for understanding the long-term cognitive risks associated with gestational cannabinoid use and reinforces clinical warnings against the use of both THC and CBD during pregnancy.

Declarations

Author Contributions: A.C.-R.: conceptualization, data curation, formal analysis, validation, writing (review and editing). D.I.: data curation, writing (review and editing). O.L.: D: data curation, formal analysis. S.W: formal analysis; P.C.: conceptualization, methodology, project administration, supervision. O.J.J.M.: conceptualization, supervision, funding acquisition, methodology, project administration, writing (original draft, review, and editing). All authors have read and agreed to the published version of the manuscript.

Declarations of interest: The authors declare no competing interests.

Funding and Disclosures: This work was supported by the Institut National de la Santé et de la Recherche Médicale (INSERM U1249), the IReSP and INCa in the framework of a call for doctoral grant applications launched in 2022 (SPADOC22-003), IReSP-AAPSPS2022-V3-05 in the framework of a call for projects to combat the use of and addiction to psychoactive substances launched in 2022 and Initiative d'Excellence d'Aix-Marseille Université – AMIDEX, grant no. AMX-22-CEX-057. This work was supported by the 2025 NRJ-Institut de France Prize in Neuroscience awarded to O.J.M.

Acknowledgements: The authors are grateful to the Chavis-Manzoni team members for helpful discussions. The authors would like to acknowledge the use of the large language model Gemini (Google) for structural and linguistic refinements.

References

1. Scheyer AF, Melis M, Trezza V, Manzoni OJJ. Consequences of Perinatal Cannabis Exposure. Trends Neurosci. 2019;42(12):871–84. doi:10.1016/j.tins.2019.08.010 PubMed PMID: 31604585; PubMed Central PMCID: PMC6981292.
2. Sarikahya MH, Cousineau SL, De Felice M, Szkudlarek HJ, Wong KKW, DeVuono MV, et al. Prenatal THC exposure induces long-term, sex-dependent cognitive dysfunction associated with lipidomic and neuronal pathology in the prefrontal cortex-hippocampal network. Mol Psychiatry. 2023;28(10):4234–50. doi:10.1038/s41380-023-02190-0 PubMed PMID: 37525013.
3. Bara A, Ferland JMN, Rompala G, Szutorisz H, Hurd YL. Cannabis and synaptic reprogramming of the developing brain. Nat Rev Neurosci. 2021;22(7):423–38. doi:10.1038/s41583-021-00465-5 PubMed PMID: 34021274; PubMed Central PMCID: PMC8445589.
4. Manzoni OJ, Manduca A, Trezza V. Therapeutic potential of cannabidiol polypharmacology in neuropsychiatric disorders. Trends Pharmacol Sci. 2025;46(2):145–62. doi:10.1016/j.tips.2024.12.005 PubMed PMID: 39837749.
5. Manduca A, Trezza V. Chapter 5 - Behavioral consequences of pre/peri-natal Cannabis exposure. In: Cannabis and the Developing Brain. Academic Press; 2022. p. 79–94. doi:10.1016/B978-0-12-823490-7.00014-9
6. Harkany T, Guzmán M, Galve-Roperh I, Berghuis P, Devi LA, Mackie K. The emerging functions of endocannabinoid signaling during CNS development. Trends Pharmacol Sci. 2007;28(2):83–92. doi:10.1016/j.tips.2006.12.004 PubMed PMID: 17222464.
7. Harkany T, Cinquina V. Physiological Rules of Endocannabinoid Action During Fetal and Neonatal Brain Development. Cannabis Cannabinoid Res. 2021;6(5):381–8. doi:
10.
1089/can.2021.0096 PubMed PMID: 34619043; PubMed Central PMCID: PMC8664114.
8. Manduca A, Servadio M, Melancia F, Schiavi S, Manzoni OJ, Trezza V. Sex-specific behavioural deficits induced at early life by prenatal exposure to the cannabinoid receptor agonist WIN55, 212-2 depend on mGlu5 receptor signalling. Br J Pharmacol. 2020;177(2):449–63. doi:10.1111/bph.14879 PubMed PMID: 31658362; PubMed Central PMCID: PMC6989958.

9. Bara A, Manduca A, Bernabeu A, Borsoi M, Serviado M, Lassalle O, et al. Sex-dependent effects of in utero cannabinoid exposure on cortical function. Elife. 2018;7:e36234. doi:10.7554/eLife.36234 PubMed PMID: 30201092; PubMed Central PMCID: PMC6162091.
10. Vargish GA, Pelkey KA, Yuan X, Chittajallu R, Collins D, Fang C, et al. Persistent inhibitory circuit defects and disrupted social behaviour following in utero exogenous cannabinoid exposure. Mol Psychiatry. 2017;22(1):56–67. doi:10.1038/mp.2016.17 PubMed PMID: 26976041; PubMed Central PMCID: PMC5025333.
11. Frau R, Miczán V, Traccis F, Aroni S, Pongor CI, Saba P, et al. Prenatal THC exposure produces a hyperdopaminergic phenotype rescued by pregnenolone. Nat Neurosci. 2019;22(12):1975–85. doi:10.1038/s41593-019-0512-2 PubMed PMID: 31611707; PubMed Central PMCID: PMC6884689.
12. Scheyer AF, Borsoi M, Pelissier-Alicot AL, Manzoni OJJ. Maternal Exposure to the Cannabinoid Agonist WIN 55,12,2 during Lactation Induces Lasting Behavioral and Synaptic Alterations in the Rat Adult Offspring of Both Sexes. eNeuro. 2020;7(5):ENEURO.0144-20.2020. doi:10.1523/ENEURO.0144-20.2020 PubMed PMID: 32868310; PubMed Central PMCID: PMC7540927.
13. Scheyer AF, Borsoi M, Pelissier-Alicot AL, Manzoni OJJ. Perinatal THC exposure via lactation induces lasting alterations to social behavior and prefrontal cortex function in rats at adulthood. Neuropsychopharmacology. 2020;45(11):1826–33. doi:10.1038/s41386-020-0716-x PubMed PMID: 32428929; PubMed Central PMCID: PMC7608083.
14. Swenson KS, Gomez Wulschner LE, Hoelscher VM, Folts L, Korth KM, Oh WC, et al. Fetal cannabidiol (CBD) exposure alters thermal pain sensitivity, problem-solving, and prefrontal cortex excitability. Mol Psychiatry. 2023;28(8):3397–413. doi:10.1038/s41380-023-02130-y PubMed PMID: 37433966; PubMed Central PMCID: PMC10618089.
15. Iezzi D, Caceres-Rodriguez A, Chavis P, Manzoni OJJ. In utero exposure to cannabidiol disrupts select early-life behaviors in a sex-specific manner. Transl Psychiatry. 2022;12(1):501. doi:10.1038/s41398-022-02271-8 PubMed PMID: 36470874; PubMed Central PMCID: PMC9722662.
16. Maciel I de S, Abreu GHD de, Johnson CT, Bonday R, Bradshaw HB, Mackie K, et al. Perinatal CBD or THC Exposure Results in Lasting Resistance to Fluoxetine in the Forced Swim Test: Reversal by Fatty Acid Amide Hydrolase Inhibition. Cannabis Cannabinoid Res. 2022;7(3):318–27. doi:10.1089/can.2021.0015 PubMed PMID: 34182795; PubMed Central PMCID: PMC9225394.
17. Iezzi D, Cáceres-Rodríguez A, Pereira-Silva J, Chavis P, Manzoni OJJ. Gestational CBD Shapes Insular Cortex in Adulthood. Cells. 2024;13(17):1486. doi:10.3390/cells13171486 PubMed PMID: 39273056; PubMed Central PMCID: PMC11394289.
18. Iezzi D, Cáceres-Rodríguez A, Chavis P, Manzoni OJ. Sex-specific disruptions in the developmental trajectory of anxiety-like behaviors due to prenatal cannabidiol exposure. Transl Psychiatry. 2025;15(1):354. doi:10.1038/s41398-025-03517-x PubMed PMID: 41053015; PubMed Central PMCID: PMC12500939.
19. Bara A, Manduca A, Bernabeu A, Borsoi M, Serviado M, Lassalle O, et al. Sex-dependent effects of in utero cannabinoid exposure on cortical function. eLife. 2018;7:3–5. doi:
10.
7554/eLife.36234 PubMed PMID: 30201092.
20. Iezzi D, Cáceres-Rodríguez A, Chavis P, Manzoni OJ. Sex-specific disruptions in the developmental trajectory of anxiety-like behaviors due to prenatal cannabidiol exposure. Transl Psychiatry. 2025;15(1):354. doi:10.1038/s41398-025-03517-x PubMed PMID: 41053015; PubMed Central PMCID: PMC12500939.
21. Thomazeau A, Lassalle O, Iafrati J, Souchet B, Guedj F, Janel N, et al. Prefrontal deficits in a murine model overexpressing the down syndrome candidate gene dyrk1a. J Neurosci. 2014;34(4):1138–47. doi:10.1523/JNEUROSCI.2852-13.2014 PubMed PMID: 24453307; PubMed Central PMCID: PMC3953590.
22. Lafourcade M, Larrieu T, Mato S, Duffaud A, Sepers M, Matias I, et al. Nutritional omega-3 deficiency abolishes endocannabinoid-mediated neuronal functions. Nat Neurosci. 2011;14(3):345–50. doi:10.1038/nn.2736 PubMed PMID: 21278728.
23. Jung KM, Sepers M, Henstridge CM, Lassalle O, Neuhofer D, Martin H, et al. Uncoupling of the endocannabinoid signalling complex in a mouse model of fragile X syndrome. Nat Commun. 2012;3:1080. doi:10.1038/ncomms2045 PubMed PMID: 23011134; PubMed Central PMCID: PMC3657999.
24. Bouamrane L, Scheyer AF, Lassalle O, Iafrati J, Thomazeau A, Chavis P. Reelin-Haploinsufficiency Disrupts the Developmental Trajectory of the E/I Balance in the Prefrontal Cortex. Front Cell Neurosci. 2016;10:308. doi:10.3389/fncel.2016.00308 PubMed PMID: 28127276; PubMed Central PMCID: PMC5226963.
25. Iafrati J, Malvache A, Gonzalez Campo C, Orejarena MJ, Lassalle O, Bouamrane L, et al. Multivariate synaptic and behavioral profiling reveals new developmental endophenotypes in the prefrontal cortex. Sci Rep. 2016;6:35504. doi:10.1038/srep35504

PubMed PMID: 27765946; PubMed Central PMCID: PMC5073243.

26. Labouesse MA, Lassalle O, Richetto J, Iafrati J, Weber-Stadlbauer U, Notter T, et al. Hypervulnerability of the adolescent prefrontal cortex to nutritional stress via reelin deficiency. Mol Psychiatry. 2017;22(7):961–71. doi:10.1038/mp.2016.193 PubMed PMID: 27843148.
27. Iezzi D, Cáceres-Rodríguez A, Strauss B, Chavis P, Manzoni OJ. Sexual differences in neuronal and synaptic properties across subregions of the mouse insular cortex. bioRxiv. 2023;2023.10.18.562844. doi:10.1101/2023.10.18.562844 PubMed PMID: 37905125; PubMed Central PMCID: PMC10614858.
28. Rodgers RJ, Dalvi A. Anxiety, defence and the elevated plus-maze. Neurosci Biobehav Rev. 1997;21(6):801–10. doi:10.1016/s0149-7634(96)00058-9 PubMed PMID: 9415905.
29. de Brouwer G, Fick A, Harvey BH, Wolmarans DW. A critical inquiry into marble-burying as a preclinical screening paradigm of relevance for anxiety and obsessive-compulsive disorder: Mapping the way forward. Cogn Affect Behav Neurosci. 2019;19(1):1–39. doi:10.3758/s13415-018-00653-4 PubMed PMID: 30361863.
30. Grant KS, Petroff R, Isoherranen N, Stella N, Burbacher TM. Cannabis use during pregnancy: Pharmacokinetics and effects on child development. Pharmacol Ther. 2018;182:133–51. doi:10.1016/j.pharmthera.2017.08.014 PubMed PMID: 28847562; PubMed Central PMCID: PMC6211194.
31. Bolhuis K, Kushner SA, Yalniz S, Hillegers MHJ, Jaddoe VWV, Tiemeier H, et al. Maternal and paternal cannabis use during pregnancy and the risk of psychotic-like experiences in the offspring. Schizophr Res. 2018;202:322–7. doi:10.1016/j.schres.2018.06.067 PubMed PMID: 29983267.
32. El Marroun H, Brown QL, Lund IO, Coleman-Cowger VH, Loree AM, Chawla D, et al. An epidemiological, developmental and clinical overview of cannabis use during pregnancy. Prev Med. 2018;116:1–5. doi:10.1016/j.ypmed.2018.08.036 PubMed PMID: 30171964.
33. Blanchard DC, Griebel G, Pobbe R, Blanchard RJ. Risk assessment as an evolved threat detection and analysis process. Neurosci Biobehav Rev. 2011;35(4):991–8. doi:10.1016/j.neubiorev.2010.10.016 PubMed PMID: 21056591.
34. Thomas A, Burant A, Bui N, Graham D, Yuva-Paylor LA, Paylor R. Marble burying reflects a repetitive and perseverative behavior more than novelty-induced anxiety. Psychopharmacology (Berl). 2009;204(2):361–73. doi:10.1007/s00213-009-1466-y PubMed PMID: 19189082; PubMed Central PMCID: PMC2899706.
35. Halladay LR, Blair HT. Distinct ensembles of medial prefrontal cortex neurons are activated by threatening stimuli that elicit excitation vs. inhibition of movement. J Neurophysiol. 2015;114(2):793–807. doi:10.1152/jn.00656.2014 PubMed PMID: 25972588; PubMed Central PMCID: PMC4533059.
36. Albrechet-Souza L, Borelli KG, Brandão ML. Activity of the medial prefrontal cortex and amygdala underlies one-trial tolerance of rats in the elevated plus-maze. J Neurosci Methods. 2008;169(1):109–18. doi:10.1016/j.jneumeth.2007.11.025 PubMed PMID: 18190969.
37. Klune CB, Goodpaster CM, Gongwer MW, Gabriel CJ, An J, Chen R, et al. Developmentally distinct architectures in top-down pathways controlling threat avoidance. Nat Neurosci. 2025;28(4):823–35. doi:10.1038/s41593-025-01890-w PubMed PMID: 39972221; PubMed Central PMCID: PMC11978489.
38. Xu P, Chen A, Li Y, Xing X, Lu H. Medial prefrontal cortex in neurological diseases. Physiol Genomics. 2019;51(9):432–42. doi:10.1152/physiolgenomics.00006.2019 PubMed PMID: 31373533; PubMed Central PMCID: PMC6766703.
39. Dembrow NC, Zemelman BV, Johnston D. Temporal dynamics of L5 dendrites in medial prefrontal cortex regulate integration versus coincidence detection of afferent inputs. J Neurosci. 2015;35(11):4501–14. doi:10.1523/JNEUROSCI.4673-14.2015 PubMed PMID: 25788669; PubMed Central PMCID: PMC4363381.
40. Lee AT, Gee SM, Vogt D, Patel T, Rubenstein JL, Sohal VS. Pyramidal neurons in prefrontal cortex receive subtype-specific forms of excitation and inhibition. Neuron. 2014;81(1):61–8. doi:10.1016/j.neuron.2013.10.031 PubMed PMID: 24361076; PubMed Central PMCID: PMC3947199.
41. Martin HGS, Lassalle O, Brown JT, Manzoni OJ. Age-Dependent Long-Term Potentiation Deficits in the Prefrontal Cortex of the Fmr1 Knockout Mouse Model of Fragile X Syndrome. Cereb Cortex. 2016;26(5):2084–92. doi:10.1093/cercor/bhv031 PubMed PMID: 25750254.
42. Manduca A, Bara A, Larrieu T, Lassalle O, Joffre C, Layé S, et al. Amplification of mGlu5-Endocannabinoid Signaling Rescues Behavioral and Synaptic Deficits in a Mouse Model of Adolescent and Adult Dietary Polyunsaturated Fatty Acid Imbalance. J Neurosci. 2017;37(29):6851–68. doi:10.1523/JNEUROSCI.3516-16.2017 PubMed PMID: 28630250; PubMed Central PMCID: PMC6705718.

43. Kauer JA, Malenka RC. Synaptic plasticity and addiction. Nat Rev Neurosci. 2007;8(11):844–58. doi:10.1038/nrn2234 PubMed PMID: 17948030.
44. Rodgers RJ, Dalvi A. Anxiety, defence and the elevated plus-maze. Neurosci Biobehav Rev. 1997;21(6):801–10. doi:10.1016/s0149-7634(96)00058-9 PubMed PMID: 9415905.
45. Walf AA, Frye CA. The use of the elevated plus maze as an assay of anxiety-related behavior in rodents. Nat Protoc. 2007;2(2):322–8. doi:10.1038/nprot.2007.44 PubMed PMID: 17406592; PubMed Central PMCID: PMC3623971.
46. Holly KS, Orndorff CO, Murray TA. MATSAP: An automated analysis of stretch-attend posture in rodent behavioral experiments. Sci Rep. 2016;6:31286. doi:10.1038/srep31286 PubMed PMID: 27503239; PubMed Central PMCID: PMC4977506.
47. Martin HGS, Lassalle O, Manzoni OJ. Differential Adulthood Onset mGlu5 Signaling Saves Prefrontal Function in the Fragile X Mouse. Cereb Cortex. 2017;27(12):5592–602. doi:10.1093/cercor/bhw328 PubMed PMID: 27797833.
48. Bosch-Bouju C, Larrieu T, Linders L, Manzoni OJ, Layé S. Endocannabinoid-Mediated Plasticity in Nucleus Accumbens Controls Vulnerability to Anxiety after Social Defeat Stress. Cell Rep. 2016;16(5):1237–42. doi:10.1016/j.celrep.2016.06.082 PubMed PMID: 27452462.

Figures

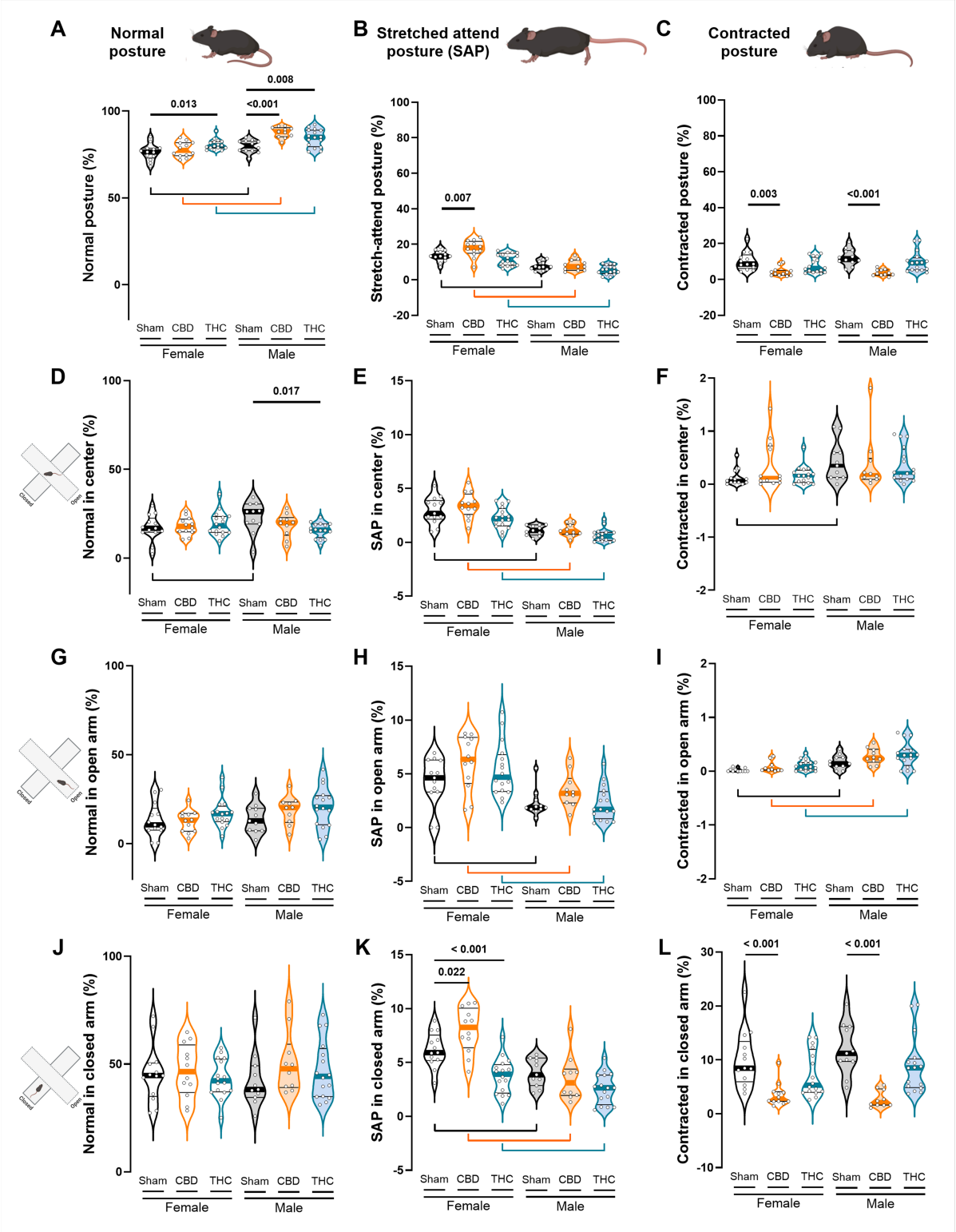

Figure 1

Prenatal exposure to CBD, but not THC, selectively enhances risk assessment behavior in adult female offspring. Postural analysis during the EPM task categorized behavior into three distinct states: normal posture (A), stretched-attend posture (SAP; B), and contracted posture (C). (A) Female offspring exposed to prenatal THC exhibited a higher prevalence of normal posture. (B) Analysis revealed that CBD-exposed females spent significantly more time in SAP compared to both Sham females and CBD-exposed males — an effect absent in THC-exposed groups. Female offspring in general display higher incidence of SAP than males, this is preserved across within treatment sex comparisons (C) CBD-exposed animals also spent less time in contracted posture, consistent with an increased expression of SAP-related risk assessment behavior. Statistical comparisons were performed using two-way ANOVA followed

by Šídák's multiple comparisons test. (D–L) Quantitative analysis of postural states, normal, contracted, and stretched-attend posture (SAP), across the three zones of the EPM revealed that, regardless of sex or prenatal treatment, both Sham and CBD-exposed offspring spent significantly more time in normal posture within the closed arms compared to the open and center arms. Notably, CBD-exposed progeny, particularly females, exhibited elevated SAP rates specifically from the closed arms prior to center entry. Data are presented as violin plots (median, and 25th–75th percentiles), with each point representing an individual animal. Statistical analysis was performed using two-way ANOVA followed by Šídák's multiple comparisons test. *P values < 0.05 are indicated in the graph. Group sizes were as follows: Sham female (N = 13), CBD female (N = 12), THC female (N = 16), Sham male (N = 11), CBD male (N = 10), THC male (N = 16).

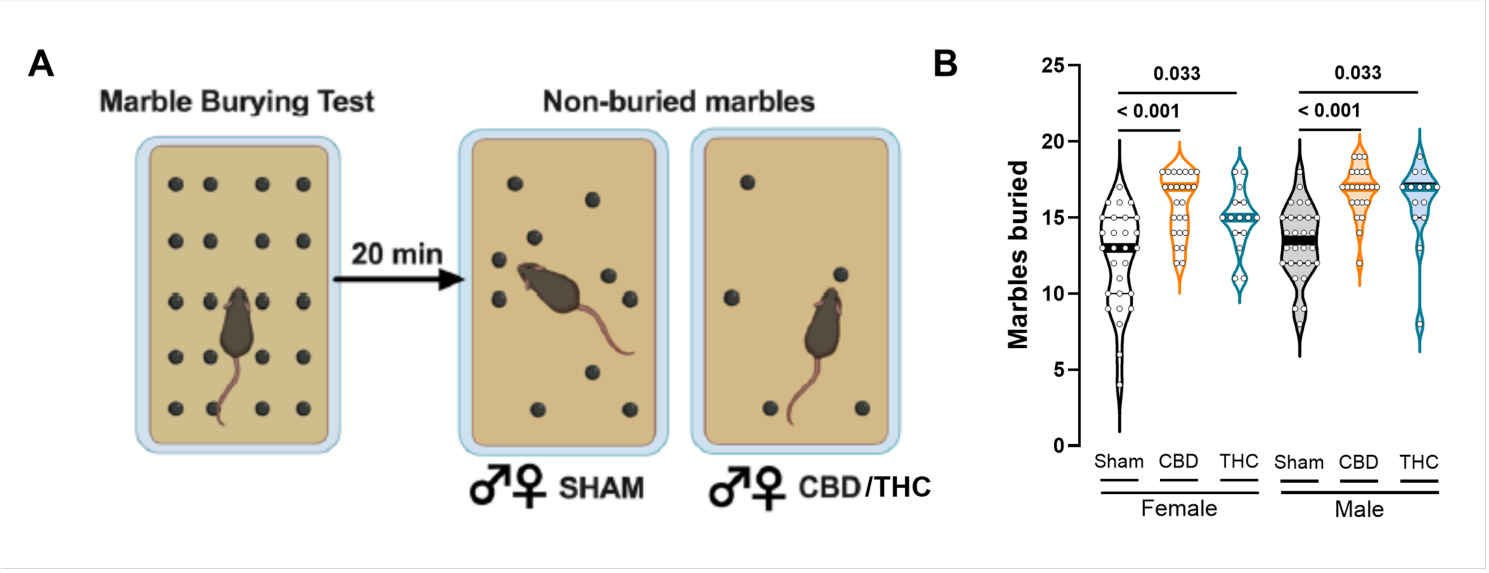

Figure 2

Gestational Cannabinoid Exposure Elevates Repetitive Responses in the Marble Burying Task. (A) Left: schematic representation of the marble burying paradigm. Right: representative results from Sham, CBD-, and THC-exposed animals of both sexes. (B) Quantification of buried marbles revealed that both male and female offspring prenatally exposed to CBD or THC buried significantly more marbles than their Sham counterparts. Data are presented as violin plots (median, and 25th–75th percentiles), with each point representing an individual animal. Statistical analysis was performed using two-way ANOVA followed by Šídák's multiple comparisons test. *P values < 0.05 are indicated in the graph. Group sizes were as follows: Sham female (N = 28), CBD female (N = 25), THC female (N = 15), Sham male (N = 28), CBD male (N = 23), THC male (N = 14).

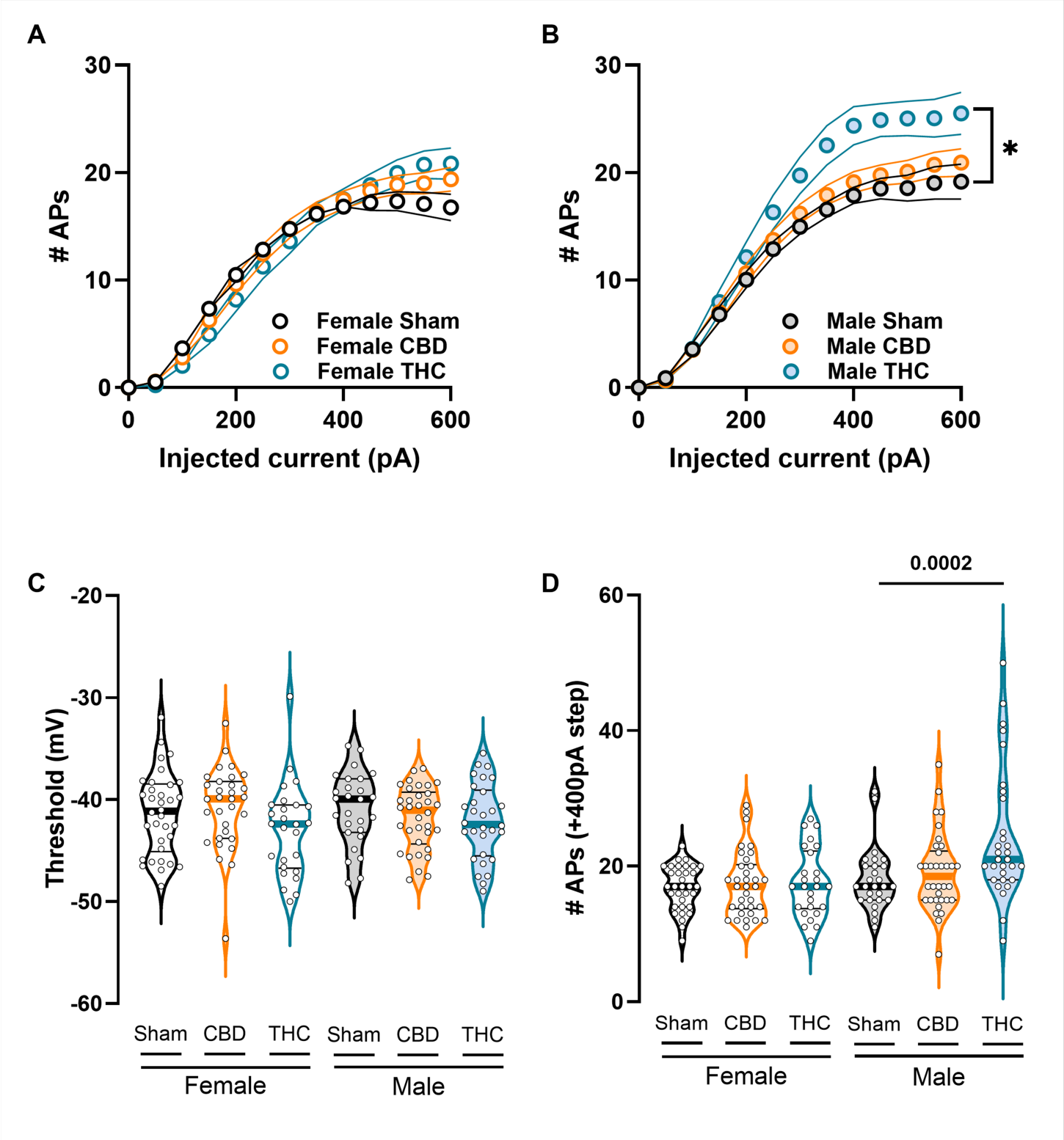

Figure 3

THC-exposed male progeny displays increased intrinsic neuronal excitability in adulthood. (A–B) Number of evoked action potentials in response to increasing depolarizing current injections. (A) Female offspring display comparable intrinsic excitability across experimental conditions. (B) Progressive depolarizing current injections (50-pA steps) reveal increased firing in THC-exposed males at supraphysiological stimulation intensities. (C) Despite this increase in firing, the action potential threshold does not differ across sex or treatment. (D) Representative example showing the number of spikes elicited by a +400-pA depolarizing current step, illustrating enhanced firing in THC-exposed males. (A–B) Each dot represents the group mean value at the corresponding current step; data are presented as mean ± SEM in XY plots and were analyzed using multiple measures Mann-Whitney Test. (C–D) Each dot represents a

single neuron; data are shown as violin plots (median, and 25th–75th percentiles) and were analyzed using two-way ANOVA followed by Šídák's multiple-comparison test. Only statistically significant differences ($p < 0.05$) are indicated in the graphs. Sample sizes (# neurons / # animals) were females Sham (34/9), CBD (31/10), THC (26/9); males Sham (27/8), CBD (34/14), THC (30/8).

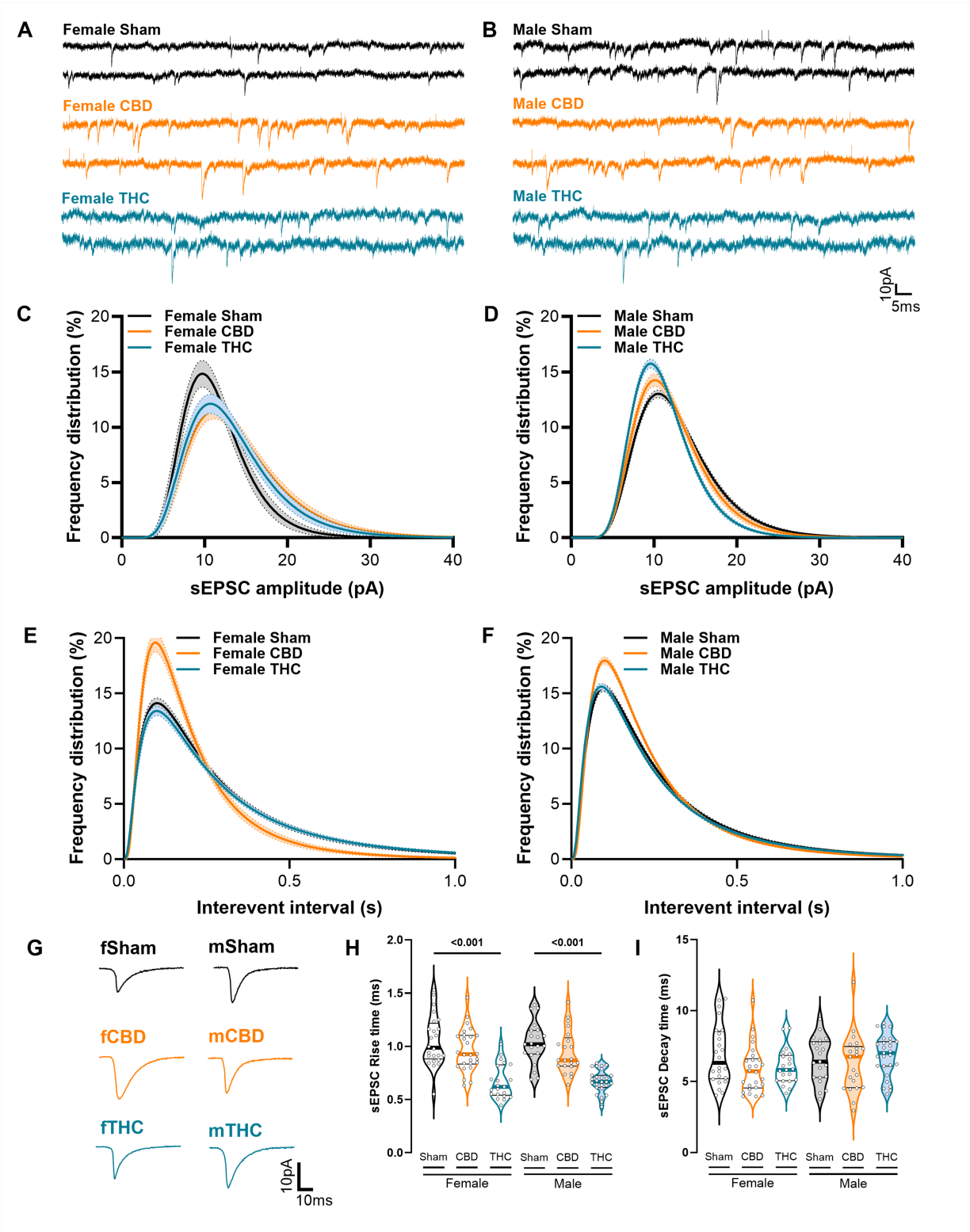

Figure 4

Prenatal cannabinoid exposure alters excitatory synaptic transmission in female progeny: (A–B) Representative traces of spontaneous excitatory postsynaptic currents (sEPSCs) recorded at −70 mV in presence of gabazine (10μM) from Sham-, CBD-, and THC-exposed female and male offspring (scale bar 10pA/5ms). (C) Log-normal distribution fitting (± CI) reveals a higher proportion of large-amplitude events in cannabinoid-treated females, whereas (D) cannabinoid-treated males display a shift toward smaller-amplitude events. (E)

IInter-event intervals are reduced in CBD-exposed females relative to Sham and THC females. (F) A higher proportion of CBD-exposed males exhibit shorter inter-event intervals, indicating increased event frequency. (G) Representative traces of averaged excitatory transmission currents. (H) Regardless of sex, THC-exposed progeny exhibits faster rise times of excitatory postsynaptic currents. (I) Decay times of excitatory postsynaptic currents remain unchanged across sex and treatment. (C-F) Data were analyzed using log-normal curve fitting with confidence intervals (± CI). (H, I) Data are presented as violin plots (median, and 25th–75th percentiles) and were analyzed using two-way ANOVA followed by Šídák's correction for multiple comparisons. Only statistically significant differences ($p < 0.05$) are indicated in the graphs additional statistical information can be found in Table 9. Sample sizes (# neurons / # animals) were females Sham (24/9), CBD (26/12), THC (21/9); males Sham (21/8), CBD (21/13), THC (27/8).

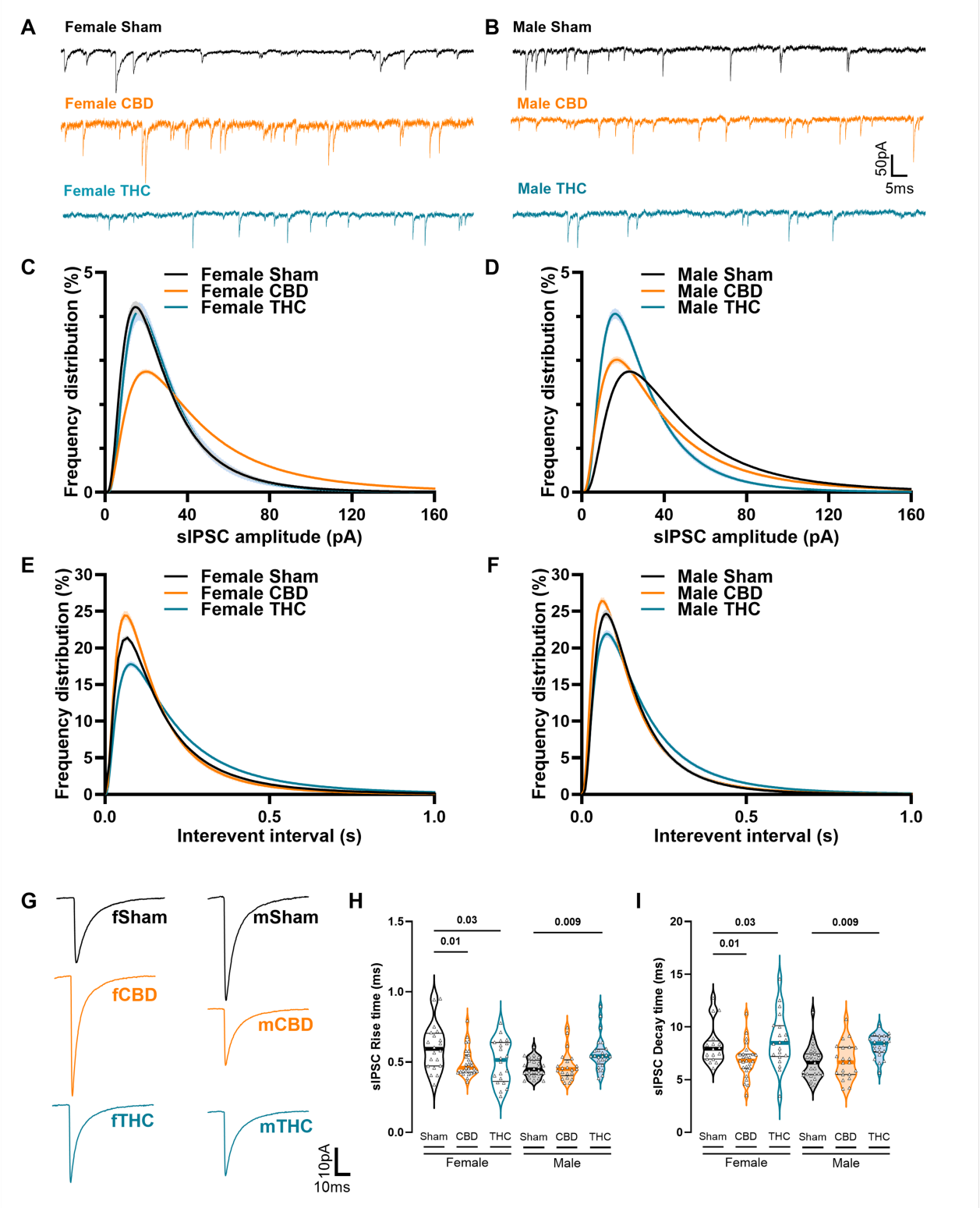

Figure 5

Prenatal cannabinoid exposure differentially alters inhibitory synaptic transmission in female and male progeny: (A–B) Representative traces of spontaneous inhibitory postsynaptic currents (sIPSCs) recorded at −70 mV from Sham-, CBD-, and THC-exposed female and male offspring in the presence of APV and CNQX (10 μM), (scale bars: 50 pA, 5 ms). (C) Log-normal distribution fitting (± CI) reveals a higher proportion of large-amplitude events in CBD-treated females, whereas (D) cannabinoid-treated males display a shift toward smaller-amplitude events. (E) In the distributions, inter-event intervals are reduced in CBD-exposed females relative to Sham and THC females. (F) Conversely, THC-exposed males display a higher proportion of longer inter-event intervals, indicative of reduced event frequency. (G) Representation on mean sIPSC currents per sex and treatment. (H) Compared with controls, inhibitory postsynaptic currents display faster rise times in cannabinoid-treated females, whereas cannabinoid-treated males exhibit slower rise times. (I) For inhibitory current decay kinetics, CBD-exposed females show faster decay times, while THC-exposed females exhibit prolonged decays; THC-exposed males also display increased decay times. (C-F) The graphs display the relative distribution of all events during 6 min recording, these data were analyzed using log-normal curve fitting with confidence intervals (± CI). (H, I) Data are presented as violin plots (median, and 25th–75th percentiles) and were analyzed using two-way ANOVA followed by Šídák's correction for multiple comparisons. Only statistically significant differences ($p < 0.05$) are indicated in the graphs. Further statistical details can be found on Table 6. Sample sizes (# neurons / # animals) were females Sham (20/6), CBD (27/7), THC (21/5); males Sham (27/7), CBD (21/7), THC (24/5).

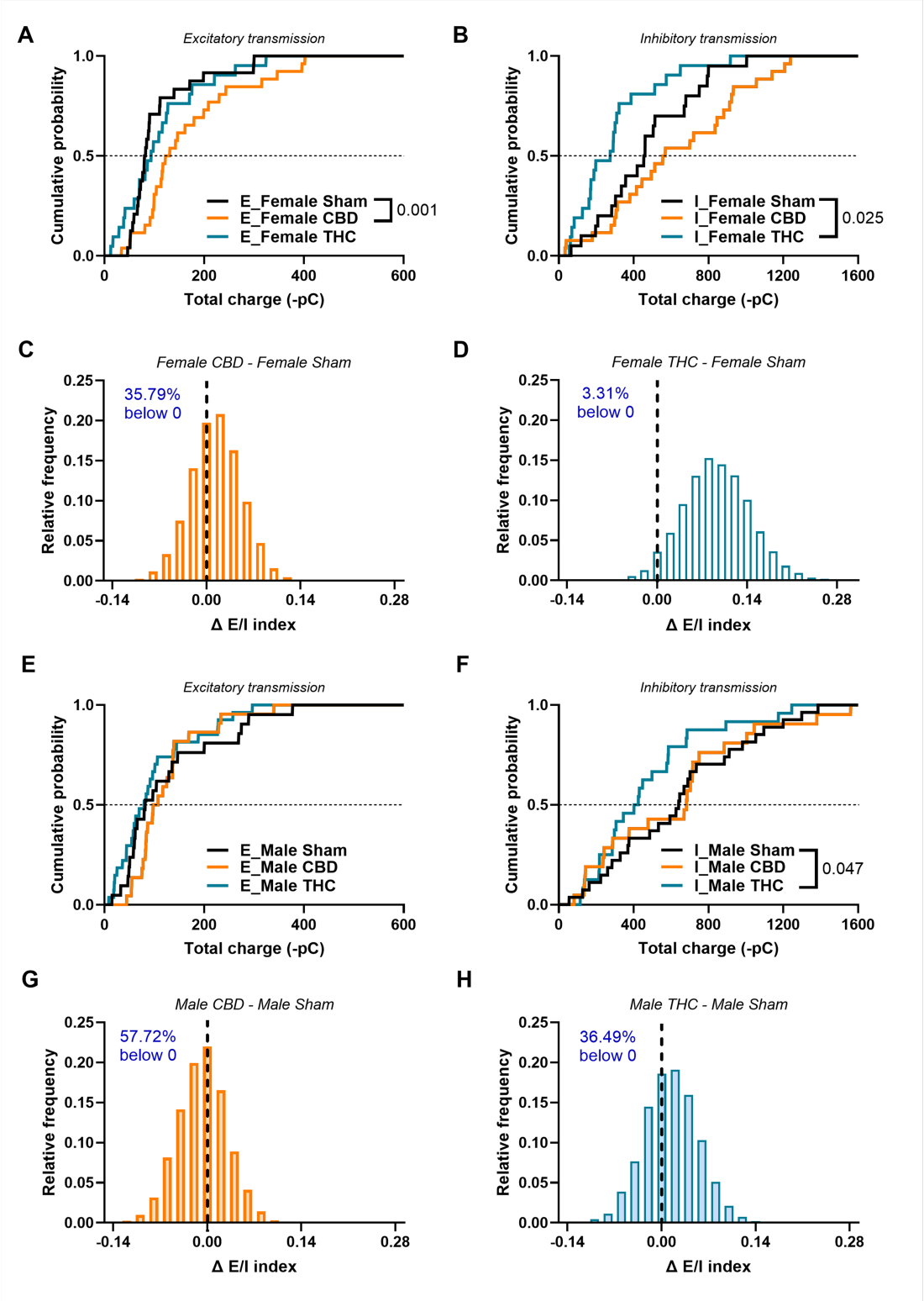

Figure 6

Prenatal cannabinoid exposure alters the excitatory/inhibitory balance. (A, E) Total charge transferred by AMPA-mediated sEPSCs and (B, F) GABA-mediated sIPSCs measured over a 6-min recording period across sexes and treatments. (A) CBD-exposed females show increased quantal excitatory transmission. (B) THC-exposed females display reduced inhibitory charge transfer compared with Sham controls. (C, D, G, H) Distribution plots of the difference between the bootstrapped E/I index of each cannabinoid-treated group and its corresponding Sham group. Distributions in which more than 95% of ΔE/I values fall on one side of zero are interpreted as significantly different ($p < 0.05$), indicating an E/I imbalance. (C) CBD-treated females show no change in E/I balance. (D) THC-treated females exhibit an increased E/I index driven by reduced inhibitory tone. (E) Total excitatory transmission remains unchanged in males, whereas (F)

THC-exposed males show a marked reduction in inhibitory charge transfer. These modest synaptic changes account for the stability of the E/I index in cannabinoid-treated male offspring. (G,H) Neither CBD- nor THC-exposed males differ from Sham in their E/I index distributions. (A,B,E,F) Cumulative frequency distributions of total charge transfer for sEPSCs (excitatory) and sIPSCs (inhibitory) were obtained from the neurons recorded in Figures 4 and 5. (C,D,G,H) Relative distribution plots show the difference between the bootstrapped E/I index of each treated group and its corresponding Sham group. Only statistically significant differences ($p < 0.05$) are indicated in the graphs. Further statistical details on the comparisons between cumulative distributions can be found on Table 11.

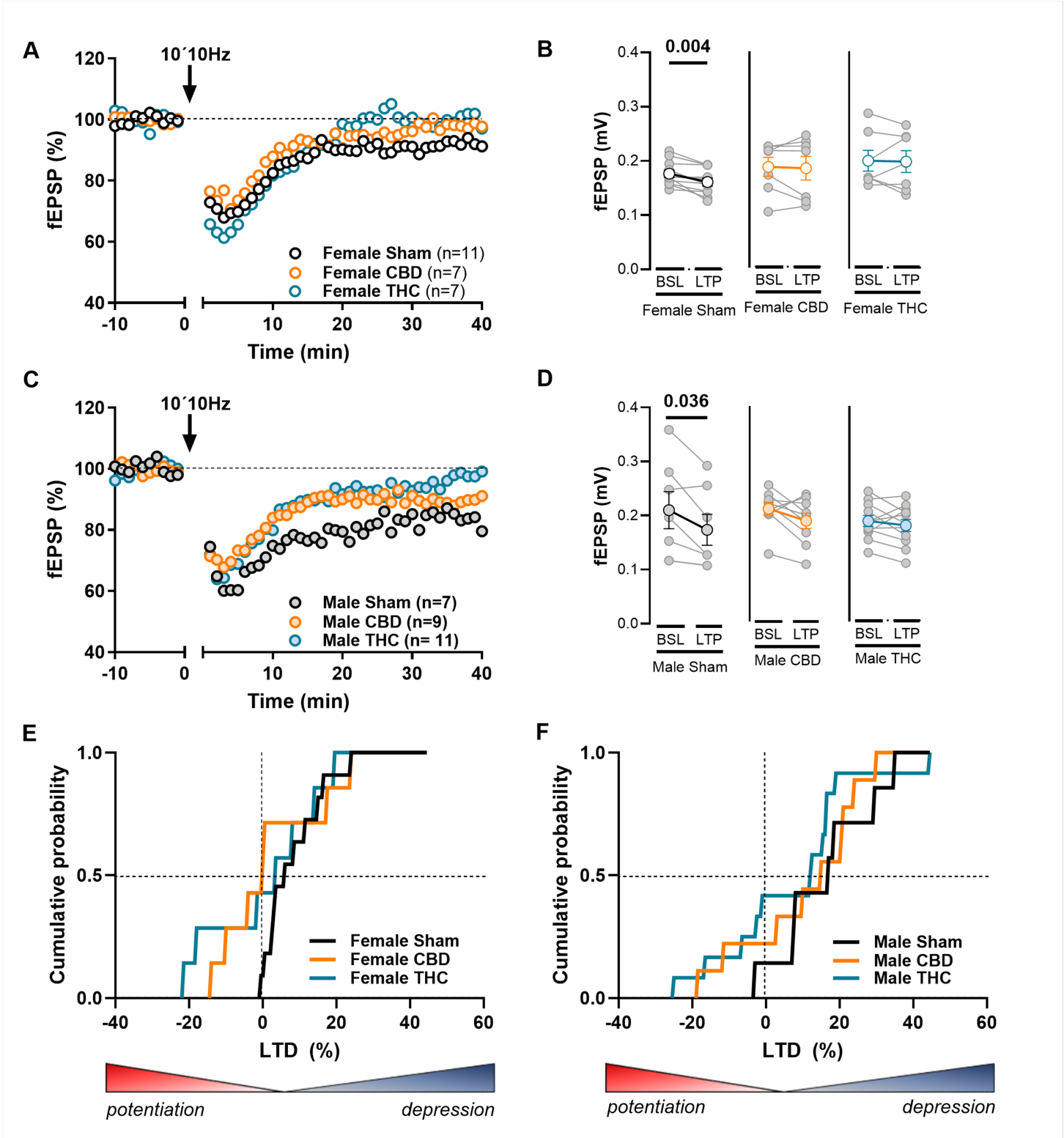

Figure 7

Prenatal cannabinoid exposure abolishes endocannabinoid-mediated long-term depression (eLTD). (A–C) Representative time courses of mean fEPSP amplitude before and after tetanic stimulation (10 × 10 Hz; arrow). (B–D) Individual experiments (grey dots) and group averages (colored circles) showing absolute fEPSP amplitudes during baseline (BSL, −10 to 0 min) and after stimulation (LTD, 30–40 min post-stimulation). Tetanic stimulation induces robust eLTD in (B) Sham females and (D) Sham males, whereas this form of synaptic plasticity is completely abolished in adult offspring prenatally exposed to CBD or THC. (E, F) Under control conditions, LTD is reliably induced in both sexes. In contrast, prenatal cannabinoid exposure abolishes LTD, with a substantial proportion of offspring instead exhibiting a potentiation response. Data are presented as mean ± SEM and were analyzed using the paired Wilcoxon test. Only statistically significant differences are indicated (*$p < 0.05$). (E, F) Cumulative probability plots show the percentage of induced LTD; negative values indicate LTP outcomes.

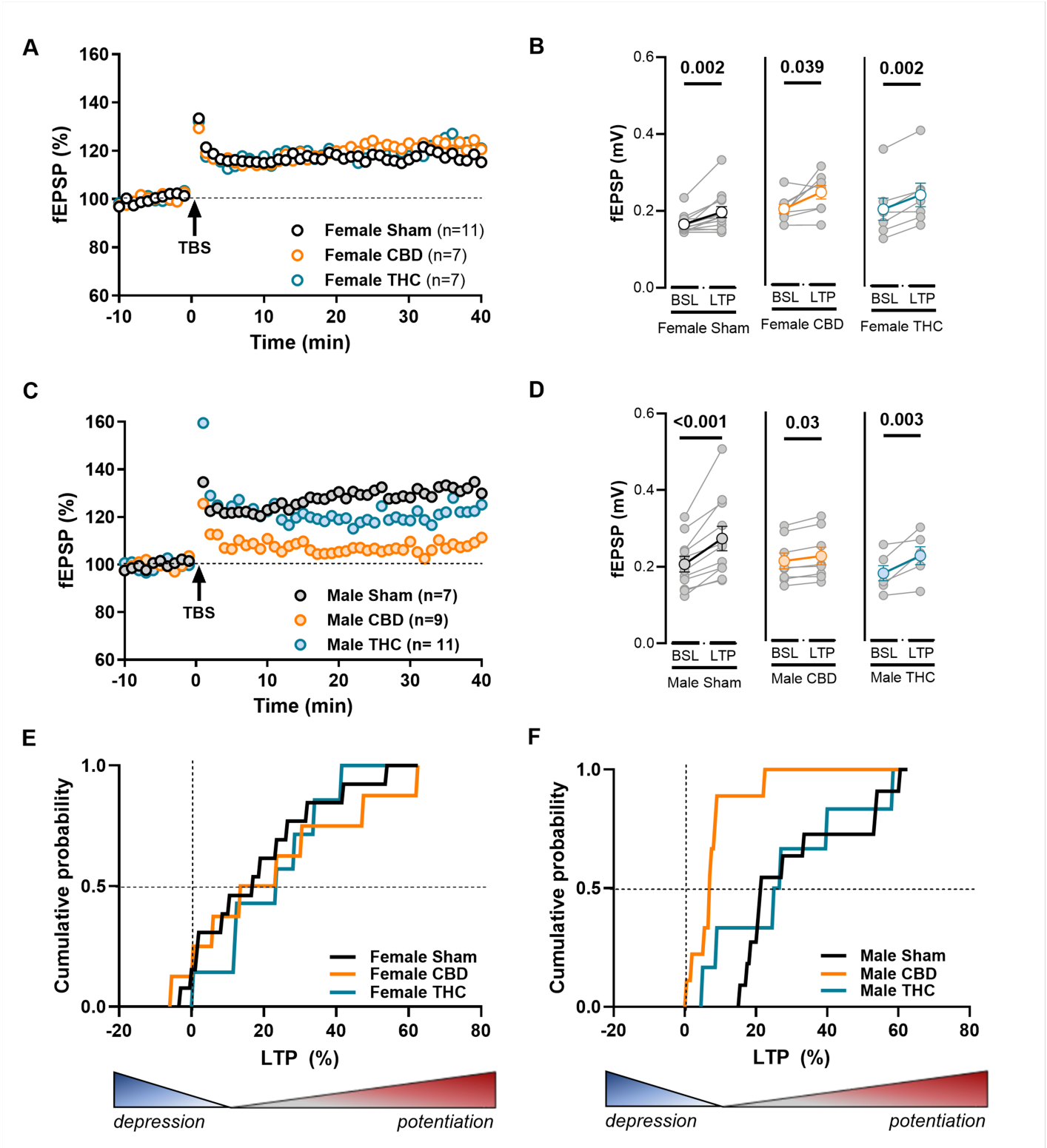

Figure 8

Prenatal cannabinoid exposure impairs long-term potentiation specifically in CBD-exposed males. (A, C) Representative time courses of normalized mean fEPSP amplitude before and after theta-burst stimulation (TBS). (B, D) Paired comparisons of mean absolute fEPSP amplitude during the 10-min baseline (BSL) versus the 30–40 min post-stimulation period (LTP). Individual experiments (grey dots) and group averages (colored circles) are shown. TBS reliably induces LTP across treatments in females (B) and in males exposed to Sham or THC (D). (E) Female offspring exposed to cannabinoids exhibit robust LTP with amplitude increases comparable to controls. (F) In contrast, CBD-exposed males show a marked reduction in LTP magnitude, with potentiation never exceeding ~20%. Data are presented as mean ± SEM and were analyzed using the paired Wilcoxon test. Only statistically significant differences are indicated (*$p < 0.05$). (E, F) Cumulative probability plots illustrate the percentage of induced LTP.

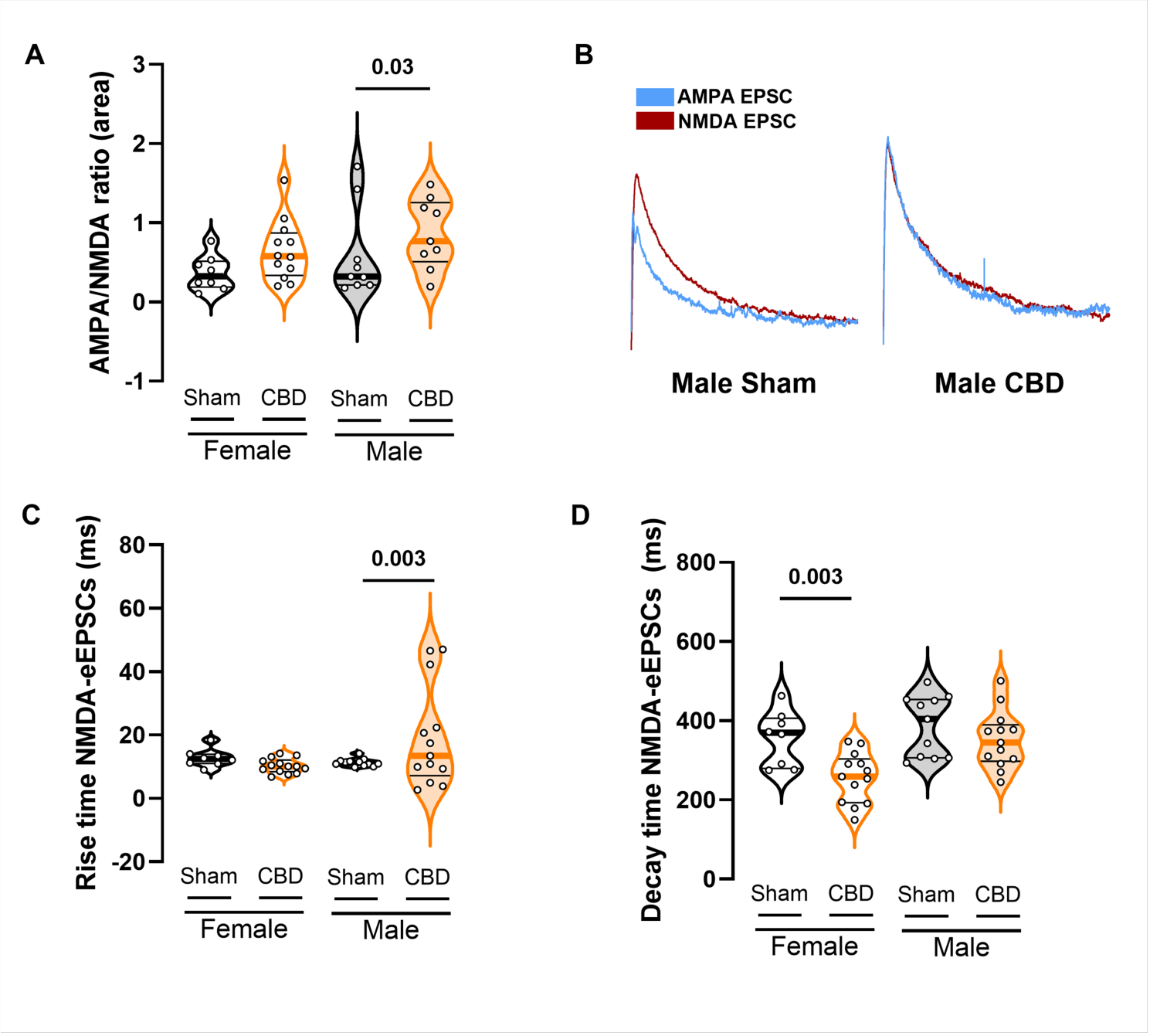

Figure 9

Selective increase in the AMPA/NMDA ratio in CBD-exposed male offspring(A) CBD-exposed males show a significant increase in the AMPA/NMDA ratio in layer V pyramidal neurons of the mPFC. (B) Representative traces of NMDA-EPSCs (red) evoked at +30 mV in the presence of 50 µM NBQX, and AMPA-EPSCs (blue) obtained by digital subtraction of the NMDA component from the dual-component

current at +30 mV. (C-D) CBD alters the kinetics of evoked NMDA currents. Male CBD-exposed offspring exhibit slower rise times, whereas CBD-exposed females display faster decay kinetics.. (A, C-D) Each point represents a single neuron; data are presented as violin plots (median and 25th–75th percentiles) and analyzed using two-way ANOVA followed by Šídák's multiple-comparison test. Only statistically significant differences ($p < 0.05$) are indicated.

Supplementary Files

This is a list of supplementary files associated with this preprint. Click to download.

- MArtSupF1.tif
- MArtSupF2IP.tif
- MArtSupF3boxplotE.tif
- MArtSupF4boxplotI.tif
- MArtSupF5.tif